DOI 10.1515/hsz-2012-0212 — Biol. Chem. 2012; 393(10): 1101–1120

**Review**

Philipp Beck**, Christian Dubiella and Michael Groll**

# Covalent and non-covalent reversible proteasome inhibition*

**Abstract:** The 20S proteasome core particle (CP) is the proteolytically active key element of the ubiquitin proteasome system that directs the majority of intracellular protein degradation in eukaryotic cells. Over the past decade, the CP has emerged as an anticancer therapy target after approval of the first-in-class drug bortezomib (Velcade®) by the US Food and Drug Administration. However, bortezomib and all second-generation CP inhibitors that are currently explored in clinical phase studies react covalently and most often irreversibly with the proteolytic sites of the CP, hereby causing permanent CP blockage. Furthermore, reactive head groups result in unspecific binding to proteasomal active centers and in substantial enzymatic off-target activities that translate to severe side effects. Thus, reversible proteasome inhibitors might be a promising alternative, overcoming these drawbacks, but are challenging with respect to their urge for thorough enthalpic and entropic optimization. This review describes developments in the hitherto neglected field of reversible proteasome inhibitors focusing on insights gained from crystal structures, which provide valuable knowledge and strategies for future directions in drug development.

**Keywords:** drug development; inhibitor; non-covalent; reversible; ubiquitin pathway.

*This paper is dedicated to Professor Robert Huber on the occasion of his 75th birthday.

****Corresponding authors: Philipp Beck and Michael Groll,** Center for Integrated Protein Science at the Department Chemie, Lehrstuhl für Biochemie, Technische Universität München Lichtenbergstraße 4, D-85747 Garching, Germany, e-mail: pbeck@mytum.de; michael.groll@mytum.de

**Christian Dubiella:** Center for Integrated Protein Science at the Department Chemie, Lehrstuhl für Biochemie, Technische Universität München Lichtenbergstraße 4, D-85747 Garching, Germany

## Introduction

Intracellular protein synthesis and degradation rank among the most essential events in living organisms. While functional analysis and structural data have significantly contributed to the recent progress in understanding the interplay between the elements of protein synthesis machineries (Ben-Shem et al., 2010), the comprehensive picture of protein degradation remains sketchy (Gallastegui and Groll, 2010). One of the most complex proteolytic pathways represents the ubiquitin proteasome system (UPS), which is strictly regulated and directs protein turnover in eukaryotic cells (Hershko and Ciechanover, 1998). The 20S proteasome core particle (CP; Figure 1A), having a molecular mass of about 720 000 Da, constitutes the central protease of the UPS. The cylinder-shaped, multimeric architecture of the CP is assembled from four stacked heptameric rings, each consisting of either α- or β-type subunits, following an $\alpha_7\beta_7\beta_7\alpha_7$ stoichiometry (Bochtler et al., 1999). The proteolytically active sites of the CP are located at the β-subunits in the inner cavity of the barrel-like structure. They all bear threonine 1 (Thr1), assigning the proteasome to the family of N-terminal nucleophilic (Ntn) hydrolases (Brannigan et al., 1995; Seemüller et al., 1995). Peptide bond breakdown in the CP occurs via the hydroxy group of Thr1 ($Thr1O^{\gamma}$), whereby the Thr1N-terminus serves as the proton acceptor (Löwe et al., 1995). In addition, a defined cluster of water molecules is placed at each active site, which functions as the proton shuttle between $Thr1O^{\gamma}$ and Thr1N (Groll and Huber, 2003). Cleavage of the scissile peptide bond is initiated by nucleophilic attack of $Thr1O^{\gamma}$ on the carbonyl carbon atom, resulting in an acyl-enzyme complex that is stabilized by the oxyanion hole. Subsequently, the ester-intermediate is hydrolyzed by a water molecule, followed by product release and regeneration of the catalytic active site. Analysis of the cleavage products at different times has revealed a processive degradation mechanism and a length distribution of oligopeptides ranging from three to 25 amino acids, thus classifying the CP as an endoprotease (Nussbaum et al., 1998). Interestingly, proteasomal digestion of proteins exhibits a stable pattern formation in the products, depending on the primary structure of the introduced substrate. Furthermore, all of the fragments generated can immediately be identified in the early process of

A

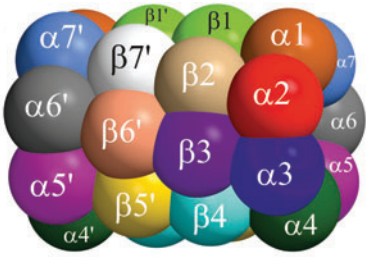


B

| Class of CP | Incorporated Subunits | | |
|---|---|---|---|
| | β1 | β2 | β5 |
| yCP | yβ1 | yβ2 | yβ5 |
| cCP | β1c | β2c | β5c |
| iCP | β1i | β2i | β5i |
| tCP | β1i | β2i | β5t |

C

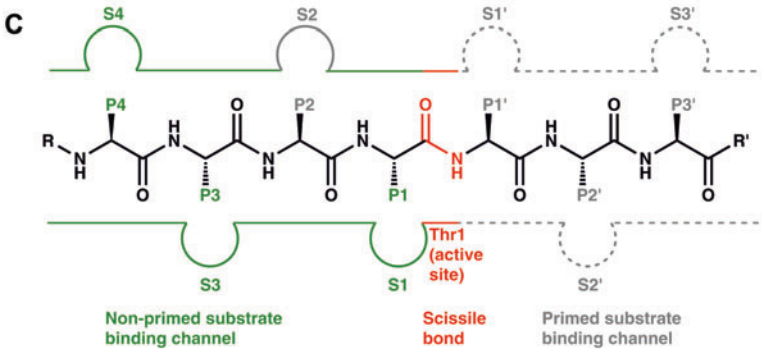


**Figure 1** Schematic representations of the topology of the 20S proteasome (CP) and the proteosomal substrate-binding channel. (A) Schematic sphere model of the quaternary structure of the CP and subtypes thereof. (B) Classes of CPs and their incorporated subunits: yeast CP (yCP), constitutive CP (cCP), immuno CP (iCP) and thymo CP (tCP). (C) General illustration of the substrate-binding channel with a peptidic ligand. The non-primed specificity pockets (S) and the interacting ligand's residues (P) are shown in green; whereas S2 is colored in gray as the proteasome lacks a prominent pocket. The primed specificity pockets (S′) have so far not been identified experimentally and are therefore drawn as gray dashed lines and the corresponding ligand's residues (P′) are in gray. The scissile peptide bond and the active site including Thr1 are highlighted in red.

turn-over. This demonstrates that the final degradation products are generated without the presence of successive large intermediates (Nussbaum et al., 1998).

Compared to archaebacterial proteasomes, which have 14 identical and 14 proteolytically active sites, eukaryotic CPs only contain three active β subunits per β ring (subunits β1, β2 and β5; Figure 1A,B) (Groll et al., 1997). Whereas the mechanism of peptide bond cleavage follows a universal principle among all CPs, it is the singularity of each substrate-binding channel that determines the chemical nature of the specificity (S) pockets and accommodates the ligand's side chains (P sites) in respect to their amino acid progression (Figure 1C). However, an individual β-subunit harboring the Thr1 still does not form an active element; it is the contribution of adjacent subunits that have a significant impact on substrate stabilization, allowing the completion of peptide bond cleavage (Groll and Huber, 2003). Although each peptide ligand adopts the formation of an antiparallel β-strand, the distinct preferences of the various active subunits were shown to be solely determined by the composition of the substrate-binding pockets, which are termed non-primed (S1, S2, S3,..., Sn) and primed (S1′, S2′, S3′,..., Sn′) sites, depending on their proximity to the active centers (Figure 1C). Residues in the substrate, which interact with the proteasomal specificity pockets, are referred to as P1, P2, P3,..., Pn and P1′, P2′, P3′,..., Pn′, accordingly (Borissenko and Groll, 2007). In agreement with ligand docking experiments, proteasomal cleavage specificities were assigned with respect to the preferred P1 amino acid of chromogenic screening substrates (Orlowski et al., 1993). Hereby, subunit β1 cleaves peptide bonds after acidic side chains, which equates to caspase-like (CL) activity. Although the β2-subunit has been attributed to trypsin-like (TL) activity, its rather large substrate binding pocket endows it with broad substrate specificity. The active sites surroundings subunit β5 are of non-polar nature and hence its substrate specificity was termed chymotrypsin-like (ChTL) activity.

The most elaborate versions of eukaryotic CPs are found in vertebrates, where three major classes of CPs shape the antigenic repertoire: the thymoproteasome (tCP) is exclusively found in cortical thymic epithelial cells, the immunoproteasome (iCP) is predominantly found in mono- and lymphocytes and the constitutive proteasome (cCP) is found in most other tissues (Rock and Goldberg, 1999; Murata et al., 2007). In addition, cytokines such as

interferon-γ (IFNγ) and tumor-necrosis factor-α induce iCP formation in cells of non-hematopoietic origin during inflammatory events (Groettrup et al., 1996). In comparison to cCPs, iCPs amplify the production of oligopeptides with hydrophobic C-termini, which are N-terminally trimmed to eight to ten amino acids, loaded on major histocompatibility complex class I (MHC-I) receptors and presented to cytotoxic T cells in order to trigger immune responses (Cascio et al., 2002). cCPs, iCPs and tCPs perform diverse biological functions, as they harbor unique sets of catalytic β-type subunits, leading to individual but overlapping peptide repertoires: cCPs incorporate the subunits β1c, β2c and β5c; iCPs the subunits β1i, β2i and β5i; and tCPs the subunits β1i, β2i and β5t. Based on their high structural similarity, both β2c and β2i are capable of generating MHC-I epitopes with neutral or basic C-terminal anchor residues (Rammensee et al., 1995). Consequently, the rationale for incorporating subunit β2i into the iCP remains elusive, and β2 subunits may play an additional, hitherto unknown functional role (Huber et al., 2012). In contrast, most residues forming the S1 specificity pocket of subunit β1c are replaced in β1i. The size of the S1 pocket is thereby reduced and the CL-activity of β1c is changed to a branched chain amino acid preferring (BrAAP) activity in β1i (Orlowski et al., 1993). Interestingly, subunits β5c and β5i are both non-polar in nature and hence, their substrate specificities were attributed to ChTL activity. Nevertheless, murine cCP and iCP crystal structures revealed that the S1 specificity pocket of β5c is significantly reduced in size compared to its β5i-counterpart (Huber et al., 2012). Therefore, β5c exerts an elastase-like or small neutral amino acid-preferring activity (SnAAP), whereas subunit β5i displays a classical ChTL activity by preferentially hydrolyzing oligopeptides C-terminally after bulky hydrophobic amino acids (Huber et al., 2012).

Participation of the proteasome in essential biological processes is well established, thus it is not surprising that academia and the pharmaceutical industry have made efforts to develop a range of natural and synthetic inhibitors against the CP. However, the immense therapeutic potential of CP inhibitors as well as the drawbacks of drugs currently applied in cancer therapies and their ineffectiveness against autoimmune diseases have proven the need for not only second-generation CP inhibitors, but also for the discovery of inhibitors with a new mechanism of action (Gräwert et al., 2011; Gallastegui et al., 2012). Irreversible ligand binding causes long-term proteasomal blockage in which the activity is only regained upon *de novo* synthesis of the CP (Schmidtke et al., 1996). In contrast, reversible inhibitors of the CP exhibit reduced side effects on healthy cells, though these compounds are still cytotoxic on rapidly dividing malignant cells. This current review covers advances in the field of reversible covalent and hitherto neglected non-covalent inhibitors of the proteasome in contrast to their irreversible counterparts. The main focus is on the comparison of structure-activity relationships (SARs) on the basis of X-ray diffraction studies of CP:ligand complexes. The mechanisms of action of various reversible inhibitors are described in detail, focusing predominantly on structural fine-tuning for enhanced binding affinity as well as selectivity. Furthermore, the molecular flexibility of distinct specificity pockets is reviewed with respect to entropic and enthalpic ligand stabilization at distinct active sites.

## The proteasome as a therapeutic target

The CP plays an essential role in disease-associated processes, such as cell proliferation, apoptosis, the regulation of gene transcription and immune response (Driscoll et al., 1993; Voorhees et al., 2003). As a result, CP inhibition leads to the accumulation of misfolded proteins and the formation of toxic reactive oxygen species in the cell. Blocking proteasome activity, however, also induces apoptosis, predominantly in malignant transformed cells that lack the ability to enter cell cycle arrest (Nawrocki et al., 2005; Bianchi et al., 2009). Furthermore, tumor cells display an elevated expression of CP resulting from defective protein synthesis in accordance with their chromosomal instability (Chauhan et al., 2010). Thus, CP inhibition shows a promising potential for drug development that was exploited by the first-in-class drug bortezomib (Figure 2E), a dipeptidyl boronic acid approved for the treatment of multiple myeloma as well as relapsed and refractory mantle cell lymphoma (Bross et al., 2003; Kane et al., 2007). Its severe adverse drug reactions include neurodegenerative effects and gastrointestinal disorders, which probably result from off-target effects against several serine proteases such as cathepsin A, cathepsin G, chymase and dipeptidyl peptidase II (Arastu-Kapur et al., 2011). Therefore, optimized second-generation CP inhibitors such as MLN2238 are currently under evaluation by the US Food and Drug Administration (Chauhan et al., 2011) (Figure 2E).

More recently, the focus of drug discovery on the CP has broadened, as selective inhibition of the iCP has demonstrated therapeutic benefit in autoimmune disorders by the downregulation of multiple proinflammatory mediators (NF-κB, interleukin-6 and tumor necrosis

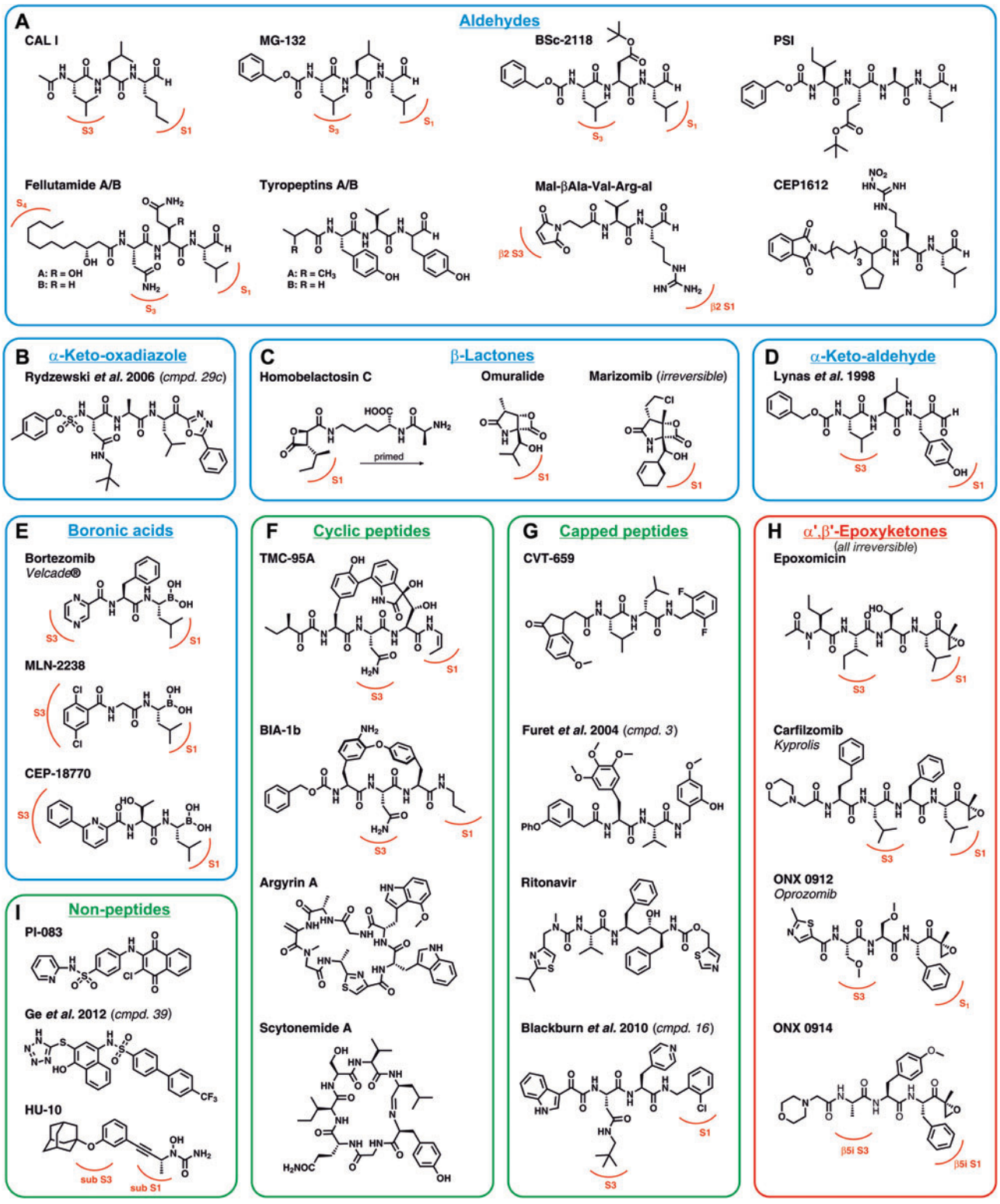


**Figure 2** Classes of proteasome inhibitors ordered by mode of action and structural characteristics.
Interactions with specificity pockets are indicated in red and termed S1, S3 and S4 (according to standard nomenclature) for compounds where a CP:inhibitor crystal structure is available. A–E (blue): reversible covalent proteasome inhibitors: aldehydes (A); α-keto-oxadiazoles (B); β-lactones (C); α-keto-aldehydes (D); and boronic acids (E). F, G, I (green): non-covalent proteasome inhibitors: cyclic peptides (F); capped peptides (G); and non-peptides (I). H (red): selection of irreversible covalent proteasome inhibitors (α′,β′-epoxyketones).

factor α; Muchamuel et al., 2009; Basler et al., 2010; Ichikawa et al., 2011). For this reason, iCP selective inhibitors such as ONX 0914 (Figure 2H) have already expanded the therapeutic spectrum (Ichikawa et al., 2011). Novel insights gained from the recently determined crystal structure of the iCP are a milestone for new avenues in structure-activity-related selective proteasome inhibition (Huber et al., 2012).

## Reversible vs. irreversible proteasome inhibition

The common design principle of proteasome inhibitors is the combination of a peptide scaffold with an electrophilic anchor, such as boronates, aldehydes, α′,β′-epoxyketones, vinyl sulfones, β-lactones, Michael systems, α-keto-1,3,4-oxadiazoles and α-ketoaldehydes (Vinitsky et al., 1992; Fenteany et al., 1995; Adams et al., 1998; Lynas et al., 1998; Nazif and Bogyo, 2001; Rydzewski et al., 2006; Groll et al., 2008; Gräwert et al., 2011). Both pharmacophoric elements, the peptide scaffold as well as the reactive head group, have an identical mode of action for all proteasomal sites and additionally modulate a plentitude of serine and cysteine proteases (Lin et al., 2009). Thus, this rather promiscuous inhibitor design is responsible for the lack of specificity, low systemic tissue distribution and severe off-target effects, as shown for bortezomib (Arastu-Kapur et al., 2011) (Figures 2E and 3C). In spite of its slowly reversible mode of action, the formation of a metastable but long-lasting covalent inhibitor-proteasome adduct is responsible for the unfavorable pharmacodynamic profile: a large fraction of the intravenously applied dose is lost due to inhibition of proteasomes in non-tumor tissue, i.e., red blood cells, liver and the vascular endothelium. While irreversible proteasome blockage is desirable and effective when targeting parasites (Prudhomme et al., 2008; Lin et al., 2009), it should not be the first choice in fighting cancer or immunologically related diseases in human because off-target effects and dose-limiting cytotoxicity against healthy cells are evident. Furthermore, cellular defense mechanisms encompass both mutations and the elevated expression of proteasomes upon treatment with irreversible or slowly reversible inhibitors, therefore inducing resistance (Franke et al., 2012; Kumar et al., 2012).

In contrast, reversible and hence time-limited proteasome inhibition without employing a reactive electrophilic anchor is suggested to exhibit increased target selectivity and be devoid of the intrinsic drawbacks associated with either irreversible or slowly reversible adduct formation. Nevertheless, from a thermodynamic and chemical point of view, the enthalpic advantage of covalent vs. non-covalent inhibitors has to be compensated by the dedicated fine-tuning of specifications such as rigidity, hydrogen bond networks, Van der Waals interactions and polarity.

## Peptide aldehydes – a versatile tool to evaluate potentials of CP inhibition

Peptide aldehydes were the first compounds investigated for proteasomal inhibition, with the most prominent example being Calpain Inhibitor I (CAL I, Ac-Leu-Leu-nLeu-al, Figures 2A and 3A). CAL I is a specific inhibitor for the ChTL activity that bears an aldehyde as the electrophilic head group on a tripeptide backbone (Wilk and Orlowski, 1983). Upon binding of CAL I and peptide aldehydes in general, the nucleophilic attack of Thr1O$^{\gamma}$ at the carbonyl carbon results in the formation of a hydrolysable and hence reversible hemiacetal (Scheme 1A), stabilized through the interactions of the newly formed tertiary hydroxy group with the oxyanion hole (Löwe et al., 1995; Groll et al., 1997). Generation of an antiparallel β-sheet of the tripeptide backbone with the substrate-binding channel provides a prolonged mean residence time of the ligand at the catalytic center and thus contributes to adduct formation. As an example, Z-Leu-al does not have any inhibitory effect, since at least a dipeptide backbone is required for stabilization of the head group near the catalytic center and subsequent formation of a covalent bond (Löwe et al., 1995). However, subunit specificity of proteasome inhibitors is not determined by the functional reactive group or the peptide backbone, but by the composition of characteristic side-chains. In the case of CAL I, the norleucine (nLeu) P1 residue resembles the hydrophobic nature of the S1 specificity pocket of β5 and additionally displaces the flexible Met45 side-chain due to steric interactions. This enlargement of the S1 pocket facilitates further Van der Waals contacts and predominantly determines the CAL I's subunit preference for ChTL activity, as the corresponding S1 pockets of the CL and TL activities both differ in size and polarity. The P2 residue projects towards the solvent and displays no interaction with the protein, yet the Leu P3 side chain shows interactions with the S3 pocket of subunit β6.

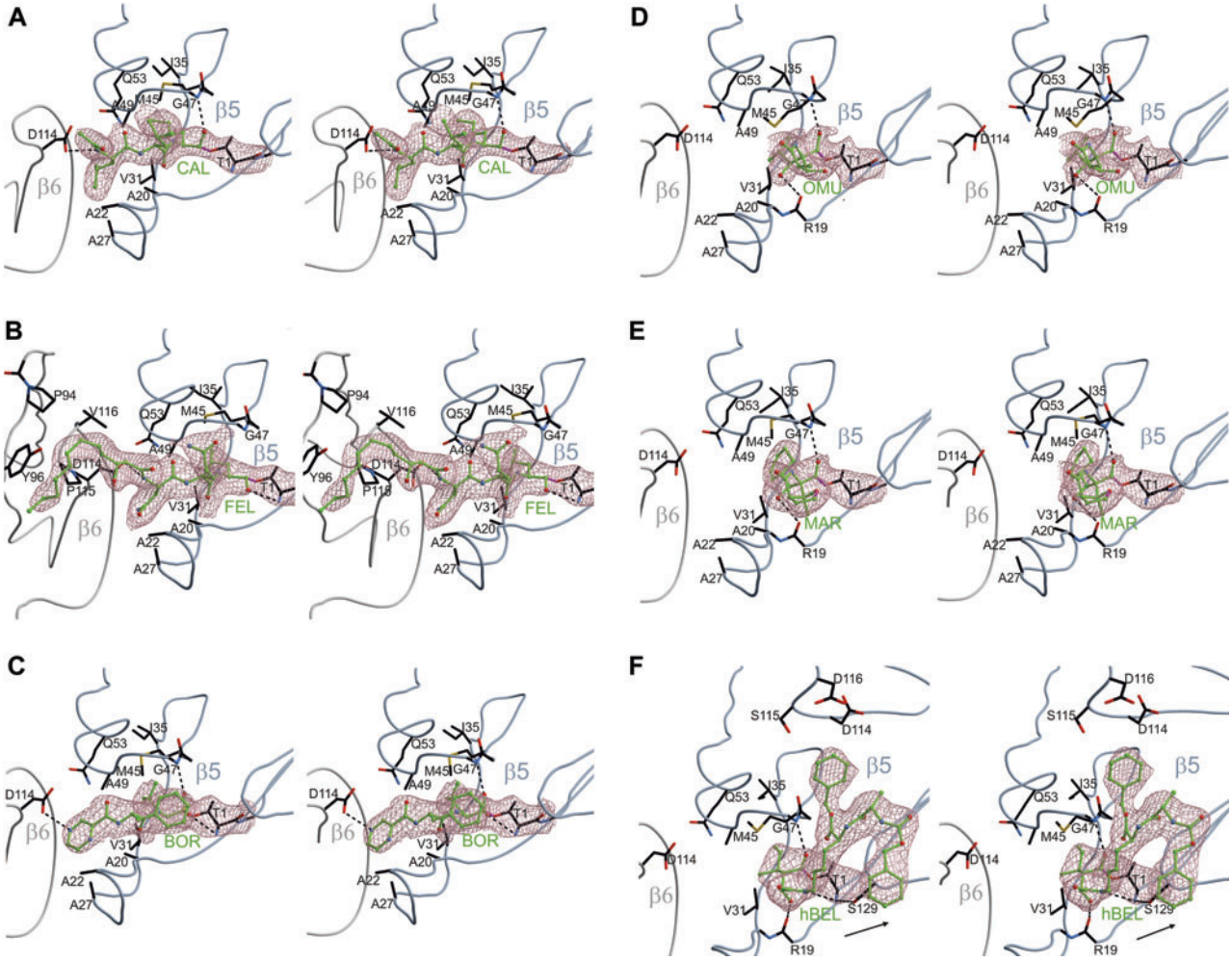


**Figure 3** Stereo representation of the electron density (red) of inhibitors (green) bound to the ChTL active site.
Hydrogen bonds are indicated by black dashed lines, 2-(*N*-morpholino)ethanesulfonic acid is cyan. The newly formed covalent bonds are shown in magenta. CP side-chains are marked in black. The arrow in the CP:homobelactosin C structure points to the primed sites. To provide good comparability, all stereo representations hold the same orientations with a fixed viewing angle. (A) Calpain Inhibitor I (CAL); (B) fellutamide B (FEL); (C) bortezomib (BOR); (D) omuralide (OMU); (E) marizomib (MAR); (F) diprotected homobelactosin C (hBEL).

As a result of CAL I's P1 side-chain, $K_i$ values indicate preferential inhibition of β5 (630 nM), whereas β1 as well as β2 are hardly affected ($K_i$>230 μM). In retrospective, peptide aldehydes largely contributed to the characterization of proteasomal proteolytically active sites. Low selectivity of CAL I for the proteasome led to further research and resulted in the far more potent and selective MG132 (Z-Leu-Leu-Leu-al; Figure 2A) (Palombella et al., 1994), which is one of the most frequently used reference CP inhibitors today. Besides alterations in their N-terminal protection groups, which are not in contact with the CP, CAL I and MG132 are constitutional isomers whose sole difference is whether the P1 residue is nLeu or Leu. However, MG132 presents an approximately eight-fold decreased $K_i$-value of 75 nM for the ChTL active site compared to 630 nM for Cal I (Table 1), which is enthalpically explained by both the ligand induced characteristic displacement of β5-Met45 and the corresponding Van der Waals interactions in the S1 pocket (P.B., C.D., M.G. personal communication).

Further examples of peptide aldehydes that have been applied as CP inhibitors include PSI (Z-Ile-Glu(O*t*Bu)-Ala-Leu-al; Figure 2A) and the dipeptide aldehyde CEP1612 (phthalimido-$(CH_2)_8$-CH-(cyclopentyl)-COArg($NO_2$)-Leu-al; Figure 2A), which both exhibit similar selectivity (Figueiredo-Pereira et al., 1994; Harding et al., 1995) (Table 1). Interestingly, BSc2118 (Z-Leu-Asp(O*t*Bu)-Leu-al; Figure 2A) displays a $K_i$ of 58 nM for β5, although it is identical to MG132 except for the P2 side-chain which is replaced by a bulky Asp(O*t*Bu) residue (Braun et al., 2005). As CPs lack a defined S2 pocket, the P2 side-chain can be utilized to prevent unspecific inhibition of proteases with

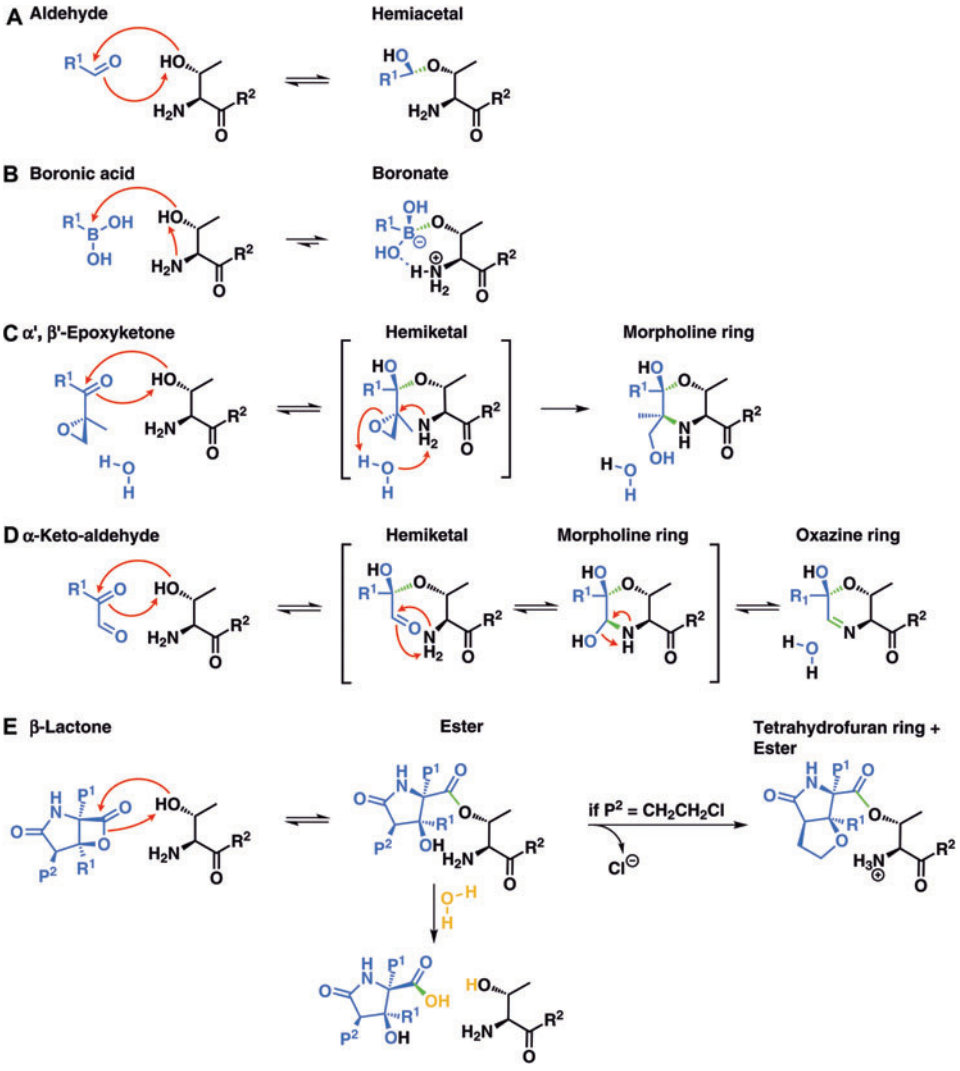


**Scheme 1** Mechanism of action of head groups that covalently react with the nucleophilic Thr1O$^{\gamma}$ of proteolytically active subunits. Aldehydes (A), boronic acids (B), α′,β′-epoxyketones (C), α-keto-aldehydes (D), and β-lactones (E) are blue. R$^1$ indicates variable residues, Thr1 is marked in black and R$^2$ denotes the main protein chain of the active β-subunit. Newly formed bonds are colored in green. P$^1$ and P$^2$ indicate variable side chains of lactone inhibitors.

well-defined S2 pockets. The CP:BSc2118 crystal structure revealed that the P2-Asp(O*t*Bu) side-chain does not form strong interactions with the protein (Braun et al., 2005). Thus, the BSc2118 ligand flexibility is restricted and unspecific off-target activities with proteases are repressed.

Whereas peptide aldehydes were successfully tailored to target different proteolytically active subunits, selectivity against other proteases proved to be problematic. Extensive studies on peptides bearing an electrophilic α-keto-1,3,4-oxadiazole head group were conducted to find more specific proteasome inhibitors (Rydzewski et al., 2006). In a first step, peptide side-chains P1–P5 were probed and optimized for ChTL inhibition using peptide vinyl sulfones that were synthetically less challenging (Nazif and Bogyo, 2001; Groll et al., 2002; Rydzewski et al., 2006). In this series, a neopentyl-Asn substituent in P3 conveyed high selectivity and affinity for subunit β5. Subsequently, the neopentyl-Asn-Ala-Leu sequence was equipped with the α-keto-1,3,4-oxadiazole head group to generate a selective, potent and slowly reversible proteasome inhibitor (Figure 2B) with nanomolar activity *in vitro* ($K_{i\,app}$=0.72 nM for β5, Table 1) as well as in the human prostate cancer cell line PC3 ($IC_{50}$=200 nM, $K_i$ not published; Rydzewski et al., 2006). Although this class of compounds was not further investigated, studies aiming to elucidate the exact binding mode remain of interest.

Peptide aldehydes have proven to be a valuable tool for analyzing the distinct proteolytic activities of the CP

| Class | Compound | Inhibitory potency against cCP-active subunits (nM) | | | CP source | References |
|---|---|---|---|---|---|---|
| | | β1 (CL) | β2 (TL) | β5 (ChTL) | | |
| Aldehydes | CAL I | $K_i$>1 800 000 | $K_i$=230 000 | $K_i$=630 | Yeast | (Kaiser et al., 2004a) |
| | MG132 | $K_i$=4500 | $K_i$=670 | $K_i$=75 | Rabbit reticulocyte | (Basse et al., 2007) |
| | BSc-2118 | $IC_{50}$=1791 | $IC_{50}$=155 | $IC_{50}$=58 | Human red blood cells | (Braun et al., 2005) |
| | PSI | n.r. | n.r. | $IC_{50}$=250 | Bovine pituitary | (Figueiredo-Pereira et al., 1994) |
| | Fellutamide B | $IC_{50}$=1200 | $IC_{50}$=2000 | $IC_{50}$=9.4 | Mammalian | (Hines et al., 2008) |
| | Tyropeptin | $IC_{50}$=68 000 | $IC_{50}$=5000 | $IC_{50}$=140 | Human HL60 | Momose et al., 2005 |
| | Mal-βAla-Val-Arg-al | $IC_{50}$>100 000 | $IC_{50}$=500 | $IC_{50}$>100 000 | Yeast | (Loidl et al., 1999a) |
| | CEP1612 | n.r. | n.r. | $IC_{50}$=60 | Recombinant *E. coli* | (Sun et al., 2001) |
| α-Keto-oxadiazole | Rydzewski et al. 2006 (*cmpd. 29c*) | $K_{i\,app}$>900 000 | $K_{i\,app}$>300 000 | $K_{i\,app}$=0.72 | Human | (Rydzewski et al., 2006) |
| β-Lactones | Belactosin C | n.r. | n.r. | $IC_{50}$=210 | Rabbit | (Asai et al., 2004) |
| | Omuralide | n.r. | n.r. | $IC_{50}$=49 | n.r. | (Feling et al., 2003) |
| | Marizomib | $IC_{50}$=330 | $IC_{50}$=26 | $IC_{50}$=2.5 | Rabbit | (Groll and Potts, 2011) |
| α-Keto-aldehyde | Lynas et al. 1998 | n.r. | n.r. | $K_i$=3.1 | Human red blood cells | (Lynas et al., 1998) |
| Boronic acids | Bortezomib | $IC_{50}$=74 | $IC_{50}$=4200 | $IC_{50}$=7 | Human | (Demo et al., 2007) |
| | MLN-2238 | $IC_{50}$=31 | $IC_{50}$=3500 | $IC_{50}$=3.4 | Human | (Kupperman et al. 2010) |
| | CEP-18770 | n.r. | n.r. | $IC_{50}$=3.8 | Human red blood cells | (Dorsey et al., 2008) |
| Cyclic peptides | TMC-95A | $K_{i\,app}$=29 | $K_{i\,app}$=819 | $K_{i\,app}$=1.1 | Human | (Yang et al., 2003) |
| | BIA-1b | $K_i$=200 000 | $K_i$=74 000 | $K_i$=5500 | Yeast | (Kaiser et al., 2004b) |
| | Argyrin A | $IC_{50}$<600 | $IC_{50}$<60 000 | $IC_{50}$<120 | Human red blood cells | (Nickeleit et al., 2008) |
| | Scytonemide A | n.r. | n.r. | $IC_{50}$=96 | Human | (Krunic et al., 2010) |
| Capped peptides | Ritonavir | n.r. | n.r. | $IC_{50}$=3000 | Mouse fibroblast | (Schmidtke et al., 1999) |
| | CVT-659 | n.r. | n.r. | $IC_{50}$=140 | n.r. | (Lum et al., 1998) |
| | Furet et al. 2004 (*cmpd. 3*) | $IC_{50}$>20 000 | $IC_{50}$>20 000 | $IC_{50}$=15 | Human | (Furet et al., 2004) |
| | Blackburn et al. 2010 (*cmpd. 16*) | $IC_{50}$>100 000 | $IC_{50}$>100 000 | $IC_{50}$=1.2 | Human red blood cells | (Blackburn et al., 2010) |
| Non-peptides | PI-083 | $IC_{50}$=4500 | $IC_{50}$=4500 | $IC_{50}$=100 | Rabbit | (Kazi et al., 2009) |
| | Ge et al. 2012 (*cmpd. 39*) | – | $IC_{50}$=1140 | $IC_{50}$=880 | Rabbit | (Ge et al., 2012) |
| | HU-10 | – | – | $IC_{50}$=340 | Yeast | (Gallastegui et al., 2012) |
| α′,β′-Epoxyketones | Epoxomicin | $K_{ass}$=50 000 | $K_{ass}$=8000 | $K_{ass}$=60 | Bovine red blood cells | (Meng et al., 1999) |
| | Carfilzomib | $IC_{50}$=2400 | $IC_{50}$=3600 | $IC_{50}$=6 | Human | (Demo et al., 2007) |
| | ONX 0912 | n.r. | n.r. | $IC_{50}$=36 | Human | (Zhou et al., 2009) |
| | ONX 0914 | $IC_{50}$=~10 000 | $IC_{50}$=~3000 | $IC_{50}$=236 | Human | (Muchamuel et al., 2009) |

**Table 1** Inhibitory potency [nM] of compounds towards the proteolytically active sites of the constitutive proteasome (cCP).
Values of the $IC_{50}$ (nM), $K_i$ (nM), $K_{i\,app}$ (nM) are given for the compounds listed. The 'CP source' column designates the species used to measure the inhibition values. Note that values can differ significantly based upon varying experimental conditions such as CP concentrations, buffer compositions or incubation temperatures. Key: –, no inhibition; ChTL, chymotrypsin-like; CL, caspase-like; TL, trypsin-like; n.r., not reported.

but have found no further application regarding therapeutic CP inhibition. These compounds are known to have fast dissociation rates and are subject to oxidation to carboxylic acids (Kisselev and Goldberg, 2001). Their inhibitory effects are therefore rapidly reversed upon removal in cell culture experiments.

## Aldehydes and β-lactones as electrophilic head groups in natural products

In the course of evolution, a variety of natural products with a reversible covalent mode of action evolved. Both tyropeptin A/B, isolated from *Kitasatospora* sp. *MK993-dF2*, as well as the marine fungal metabolite fellutamide B from *Penicillium fellutanum*, incorporate an aldehyde as the electrophilic anchor for CP inhibition (Momose et al., 2001; Hines et al., 2008) (Figures 2A and 3B). The latter was found to induce nerve growth factor secretion in cultured neurons and fibroblasts and has thus been investigated for potential neural therapeutic use. Its unusual chemical structure and preference for inhibition of β5 in favor of β1 and β2 led to X-ray diffraction studies, which revealed that the hemiacetal adduct exists in two alternative conformations, one stabilized by occupation of the oxyanion hole and the other by forming hydrogen bonds with Thr1N. Furthermore, the aliphatic fatty acid tail exhibited Van der Waals interactions with a hydrophobic cavity in β6, whereas this is not the case once bound to β1 and β2 (Hines et al., 2008). Here, structural rearrangements of the *n*-alkyl tail prevent favorable interactions and consequently account for the high affinity for subunit β5. Both events, hemiacetal formation in two distinct stabilized forms and binding via a long aliphatic tail to a so far unobserved specificity pocket, are difficult to predict in molecular modeling studies and therefore experimental data are essential for future guided drug development.

Lactacystin was the first natural proteasome inhibitor discovered to specifically block the ChTL active site and was found to undergo *in situ* cyclization to its active form, a fused β-lactone-γ-lactam ring system (clasto-lactacystin-β-lactone or omuralide, Figures 2C and 3D; Fenteany et al., 1995; Craiu et al., 1997; Dick et al., 1997). In spite of the spring-loaded nature of β-lactone ring systems, omuralide's head group is less reactive than aldehydes and cannot be solely responsible for its high potency ($IC_{50}$ ~ 49 nM for β5, Table 1). Only the combination of three distinct features enables omuralide to undergo covalent bond formation with Thr1O$^{\gamma}$ of subunit β5. A large number of hydrogen bonds with the substrate binding channel and P1 stabilization in the β5 S1 specificity pocket prolong the mean residence time at the active center, which is important for the completion of ester bond formation with Thr1O$^{\gamma}$ (Scheme 1E). Additionally, the tertiary alcohol resulting from the ring-opening reaction is responsible for displacement of the nucleophilic water molecule, which accomplishes hydrolysis of the enzyme-acyl intermediate to restore activity of Thr1O$^{\gamma}$. Deacetylation of bound omuralide is hindered since the Bürgi-Dunitz trajectory of water-addition to the carbonyl carbon atom of the ester is broken (Bürgi et al., 1973; Groll et al., 1997, 2006c,d; Groll and Potts, 2011). Thus, reformation of the β-lactone ring can only occur in the case of nucleophilic attack of the C3 hydroxy group, to recover the active form of the ligand (Scheme 1E).

An interesting approach for the conversion of a reversible into an irreversible inhibitor is exemplified by marizomib (Salinosporamide A, NPI-0052, Nereus Pharmaceuticals, Figures 2C and 3E), which is the only non-peptidic CP inhibitor that is currently evaluated in clinical trials (Feling et al., 2003; Chauhan et al., 2005; Maldonado et al., 2005). Marizomib exhibits essentially the same γ-lactam-β-lactone scaffold as omuralide, though it displays improved potency ($IC_{50}$=2.5 nM for β5, Table 1) and bears a cyclohexene ring in P1 as well as a chloroethyl group in the P2 site. The latter moiety is responsible for the irreversible mode of action, since after ester formation with Thr1O$^{\gamma}$ a second reaction occurs. Nucleophilic attack of the C3 hydroxy group and elimination of the chloride results in formation of a tetrahydrofuran ring (Scheme 1E). Consequently, the nucleophilic water molecule that is essential for deacylation is displaced and accounts for the irreversible CP inhibition (Macherla et al., 2005; Groll et al., 2006c; Manam et al., 2008). This mechanism of action impressively exhibits an evolutionary development from a rather passive P2 side-chain upon ligand binding towards active involvement resulting in an irreversible mode of action.

Surprisingly, the classic CP inhibitor design concept is completely inverted in the class of belactosins and analogues thereof. The diprotected derivative of homobelactosin C (Figures 2C and 3F) was shown to bind to the CP in a reversed, 'moon-walk' fashion, targeting the primed site of the substrate binding channel (Asai et al., 2000; Groll et al., 2006d; Korotkov et al., 2011). Similar to omuralide, attack of Thr1O$^{\gamma}$ on the electrophilic β-lactone carbonyl carbon opens the constrained lactone, but in contrast to the fused β-lactone-γ-lactam

rings the rearrangement of the resulting C4-OH is not restricted and redirects towards Arg190 to form a hydrogen bond (Figure 3F). Consequently, the extensive 4-aminocarbonyl moiety protrudes towards the spacious ChTL-primed binding site and hydrolysis of the newly formed Thr1O$^{\gamma}$-CO ester is prevented by displacement of the nucleophilic water molecule. The ChTL subunit specificity of homobelactosin C is mediated by the diprotected side-chain, which is too large to fit into the CL and TL primed binding sites. However, the binding mode of substrates at the primed substrate-binding channels still remains unknown, since homobelactosin C does not mimic the structural elements of proteasomal natural peptide substrates. Nonetheless, comparison of primary sequences of cCP and iCP active subunits revealed noteworthy alterations (Huber et al., 2012) and produced a promising perspective for the design of selective cCP and iCP inhibitors.

## Crystallographic knowledge for the development of bivalent ligands

After determination of the CP crystal structure from yeast (Groll et al., 1997), the knowledge of distances and subunit architecture enabled new advances in proteasomal drug design strategies to produce inhibitors with higher binding preference as well as better subunit and target selectivity. Therefore, a bivalent approach was undertaken to tailor a high affinity and β2 specific ligand, which forms covalent bonds to both, the Thr1O$^{\gamma}$ and the distant S3 thiol group of Cys118 of subunit β3, that is conserved among vertebrates (Loidl et al., 1999a). Initial modeling studies with CAL I as a scaffold suggested replacing the Leu P3 residue with an electrophilic βAla-maleinimide side chain. The resulting CAL I derivative blocked the TL active site with a 10-fold increase in efficiency ($IC_{50}$=13 μM), while inhibition of β5 was decreased ($IC_{50}$ >100 μM). This proved that the bivalent, intermolecular approach is a viable concept. However, the nLeu P1 moiety of the inhibitor does not reflect the chemical nature of the S1 specificity pocket of subunit β2, which bears an overall negative charge. Thus, replacing nLeu with Arg in P1 resulted in a highly β2-selective inhibitor with an $IC_{50}$ of approximately 500 nM (Table 1). The crystal structure analysis of the yeast CP:ligand complex confirmed the hemiacetal bond with the Thr1O$^{\gamma}$ of subunit β2 as well as the covalent linkage of maleimide to Cys118 of β3 by formation of a thioether (Loidl et al., 1999a). These results underline the fact that binding of the bivalent inhibitor strongly depends on the P1 residue, as hemiacetal formation is the first step in inhibitor binding. A prolonged local residence time near the proteolytic Thr1O$^{\gamma}$ is therefore required to furnish the subsequent reaction of maleimide and Cys118 of subunit β3.

Consequently, the concept of crystal structure guided bivalency was taken to the next level: minute design of spacers to connect two ligands to target two distinct active sites of the CP was shown to further increase affinity and selectivity. Polyethylene glycol linker sequences were chosen to connect the N-termini of two CAL I inhibitors due to their resistance to proteolysis and inability to form secondary structures (Loidl et al., 1999b). Remarkably, $IC_{50}$ values for these bivalent versions of CAL I improved to 20 nM. In conclusion, the overall concept was successfully transferred to homobivalent as well as heterobivalent peptide aldehyde inhibitors, which comprise two polyethylene glycol-linked compounds with different subunit specificity and thus simultaneously block distinct proteolytically active subunits, as shown for ChTL and TL activity. In spite of the promising inhibitory profile, *in vivo* potencies of these chimeric inhibitors have not yet been evaluated.

## Bivalent head groups – a perfect match for Ntn-hydrolases

The concept of bivalency to target the CP was also shown to be exploited by nature. The microbial metabolite epoxomicin ($K_{ass}$=60 nM; Figures 2H and 4A, Table 1), isolated from the actinomycete strain No. Q996-17, has a tetrapeptide backbone with an α′,β′-epoxyketone head group (Hanada et al., 1992; Meng et al., 1999). Surprisingly, the mode of action at the proteasomal active site turned out to be unique to Ntn-hydrolases, since the electrophilic carbonyl and epoxide carbon atoms are attacked by both Thr1O$^{\gamma}$ and Thr1N in a two-step reaction (Scheme 1C; Groll et al., 2000; Huber et al., 2012): first, nucleophilic attack of Thr1O$^{\gamma}$ at the α′,β′-epoxyketone's carbonyl carbon results in formation of a hemiketal that is stabilized in the oxyanion hole. Next, attack of Thr1N on the quaternary carbon opens the epoxide ring, resulting in a secondary amine, thus irreversibly completing the morpholine ring. Due to the strong inhibition profile and the sophisticated mode of action, two inhibitors with α′,β′-epoxyketone head groups are currently being evaluated in clinical studies, ONX 0912 and carfilzomib (Demo et al., 2007; Kuhn et al., 2011). Interestingly, the CP:epoxomicin complex structure revealed a 2-(*N*-morpholino)ethanesulfonic acid (MES) molecule obtained from the crystallization buffer, that

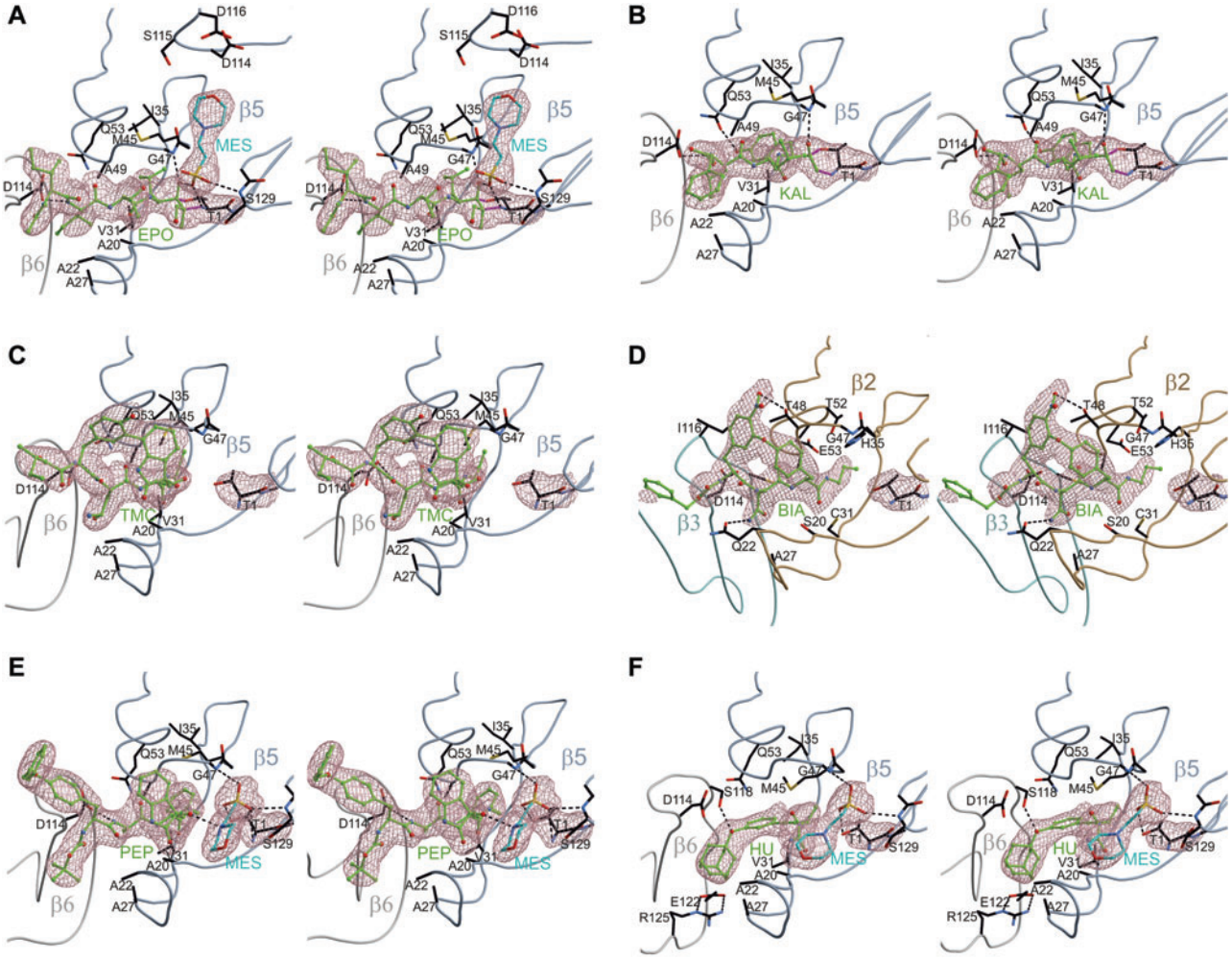


**Figure 4** Stereo representation of the electron density (red) of inhibitors (green) bound to the ChTL or TL active site.
Illustrations of compounds and CP subunits are color-coded according to Figure 3. All inhibitors shown interact with the ChTL active site except BIA-1b (BIA), which binds solely to the TL active site. (A) Epoxomicin (EPO); (B) α-keto-aldehyde (KAL); (C) TMC-95A (TMC); (D) BIA-1b (BIA); (E) decarboxylated peptide (PEP); (F) *N*-hydroxyurea compound HU-10 (HU).

resides in a similar position to the benzyl carbamate protecting group of the diprotected homobelactosin C derivative (Figures 3F and 4A). This observation indicates that this site can be further exploited for the development of ligands targeting the primed site (P.B., C.D., M.G. personal communication).

The bivalent approach is not limited to irreversible inhibition, as was shown in the case of α-keto-aldehydes, which display a similar yet reversible mode of action (Scheme 1D, Figures 2D and 4B; Lynas et al., 1998; Gräwert et al., 2001). Formation and stabilization of the hemiketal after attack of Thr1O$^{\gamma}$ proceeds as described above, nevertheless, a second step encompasses nucleophilic attack of Thr1N on the aldehyde carbon and intermediate formation of a tetrahedral carbinolamine. After condensation, a rigid 5,6-dihydro-2H-1,4-oxazine ring is formed. Additionally, a 3.0 Å hydrogen bond connecting the oxazine nitrogen with Tyr168O is observed in the crystal structure, supporting a protonated, positively charged imino nitrogen. This charge distribution facilitates hydration of the neighboring carbon center and hence contributes to reversibility of the reaction in agreement with kinetic measurements (Lynas et al., 1998; Gräwert et al., 2011). Overall, both steps towards ring formation are reversible and so are distinct from the related irreversible character of the morpholine ring upon binding of α′,β′-epoxyketone peptides (Scheme 1D). Due to the two-step reaction with both of the nucleophilic moieties of the terminal Thr1, α′,β′-epoxyketones and α-keto-aldehydes show higher selectivity than peptide aldehydes, resulting in lower off-target binding to all kinds of proteases, which as a rule lack a free N-terminus in the active center. Although *in vivo* data have not been elucidated for α-keto aldehydes, it can be expected that this class of inhibitors will be less cytotoxic than peptide

epoxyketones due to a rapidly reversible mode of action and a less reactive, hydrated head group in solution.

## Peptide boronic acids: reversible yet not ideal proteasome inhibitors

In general, boronic acid head groups are much more potent than aldehydes and have slower dissociation rates. Comparison of the widely used reference compound MG132 (Figure 2A) against its boronic acid analogue MG262 (Z-Leu-Leu-Leu-boronate) revealed that the latter displays a 100-fold improved $K_i$ value that is as low as 30 nM against the ChTL activity of rabbit proteasome (Adams et al., 1998). Good stability and bioavailability of dipeptide boronates *in vivo* led to the development of bortezomib (Figures 2E and 3C), which under physiological conditions preferentially targets the proteasomal β5 active site over β1, with β2 hardly being inhibited (Adams et al., 1999; Berkers et al., 2005). According to structural studies of the yeast CP:bortezomib complex (Groll et al., 2006a), the boron atom forms a covalent adduct with Thr1O$^{\gamma}$, while one acidic boronate hydroxy group forms a hydrogen bond with Gly47NH (Scheme 1B). To complete the tetrahedral stabilization of the head group, the residual boronic acid's hydroxy group forms a hydrogen bridge to Thr1NH. In combination with the high affinity of boron for hard over soft bases, this explains bortezomib's preference towards Ntn-hydrolases compared to cysteine proteases. The preference for subunit β5 is the result of an induced fit on a small scale, as upon antiparallel β-sheet formation the Leu P1 residue protrudes deeply into the S1 specificity pocket, similar to that observed and described for the CP:CAL I complex. Interestingly, the C-terminal pyrazine cap shows no defined interaction with the S3 pocket and thus bortezomib's overall design fails to discriminate between the cCP and iCP subtypes (β5c/β5i $IC_{50}$=7/4 nM; Table 1; Huber et al., 2012). Therefore, subunit- and target-specificity as well as pharmacokinetic and pharmacodynamic parameters have to be tuned by side-chain modification, giving rise to the second-generation peptide boronic acids that are currently in clinical trials, namely delanzomib (CEP-18770; Piva et al., 2008) and MLN2238 (Kupperman et al., 2010) (Figure 2E). MLN2238 consists of the same dipeptide backbone as bortezomib, but differs in the nature of its P2 and P3 sites: the Phe side-chain in P2 is removed in favor of Gly, while the N-terminal pyrazyl ring is replaced by a 2,5-dichlorobenzene. CEP-18770 consists of the same Leu boronic acid head group on a dipeptide scaffold, but in contrast bears a polar threonine side-chain in P2 and a substantially larger N-terminal cap. Both compounds are orally active and hence advantageous in their application (Piva et al., 2008; Kupperman et al., 2010). Interestingly, compared to bortezomib, MLN2238 and CEP-18770 also show enhanced anti-tumor activity rather than improvements in potency or subunit selectivity. MLN2238, in particular, displays enhanced sustained effects in both solid tumor and hematologic xenograft models due to better systemic tissue distribution. Improved dissociation rates ($t_{1/2}$ of 18 vs. 110 min) prevent the predominant inhibition of CPs in off-target tissue, such as red blood cells and hepatocytes, and thus avoid getting trapped immediately after application.

In summary, all compounds currently in clinical phase studies employ reactive head groups as electrophilic anchors to target the N-terminal Thr1O$^{\gamma}$. Following comparison of ONX 0914 and carfilzomib, however, it appears that functional reactive groups are not responsible for selectivity of β5c or β5i. In fact, discrimination between the immuno- and constitutive proteasome is only mediated by dedicated fine-tuning of P1–P4 residues to complement the different specificity pockets (Huber et al., 2012).

## Cyclic peptides with optimized entropic and enthalpic properties

The natural cyclic peptide TMC-95A (Figures 2F and 4C) from *Apiospora montagnei* provides an example of precisely tuned, reversible protein-ligand interactions (Koguchi et al., 2000; Groll et al., 2001). It displays a remarkable inhibitory profile due to a constrained structure and sophisticated network of hydrogen bonds between the peptide backbone and the substrate-binding channel as well as its characteristic side chains: inhibition of the ChTL-activity of human cCP with an $K_{i\,app}$ value of 1.1 nM (Table 1) demonstrates that strong potency is not a matter of employing a reactive head group (Yang et al., 2003). As revealed by structural superpositions of bound and unbound TMC-95A, no conformational alterations are observed, suggesting that the entropic penalty due to rearrangement upon binding is reduced to a minimum (Koguchi et al., 2000; Groll et al., 2001). In addition, TMC-95A does not inhibit other proteases such as m-calpain, cathepsin L and trypsin, owing to its overall architecture and side-chain design that includes a crosslink of the oxindole P2 residue with the P4 Tyr, inducing an atropisomeric system (Koguchi et al., 2000).

Approaches for a synthetically less demanding structural design retaining TMC-95A's entropic and enthalpic optimized binding mode yielded analogues with only

slight structural changes. Interestingly, removal of the hydroxy groups at the P2 side-chain and replacement of the conformationally restricted P1 *Z*-propenyl residue with a more flexible *n*-propyl revealed a 20-fold reduction of the inhibition rate for ChTL-activity (Lin and Danishefsky, 2002; Lin et al., 2004). This is explained by the enthalpic and entropic penalty, as the synthetic analogues are more flexible and lack two hydrogen-bonding hydroxy groups (Kaiser et al., 2002, 2003; Berthelot et al., 2003; Albrecht and Williams, 2004). Surprisingly, extension of the *n*-propyl P1 residue by one methylene group to gain β5 specificity resulted in a 1000-fold increased $K_i$ compared to the natural product (Kaiser et al., 2004a). This effect is caused by a steric clash of the elongated P1 nLeu side-chain with β5-Met45 and consequent disruption of the antiparallel β-sheet of the ligand and protein in the active site cleft. Displacement of the flexible β5-Met45 residue upon ligand binding is frequently observed with covalently bound inhibitors, although this plasticity of the β5 S1 pocket cannot be transferred to working hypotheses of non-covalent inhibitors. Covalently reacting inhibitors provide an additional leverage for major structural rearrangements of the β5 S1 specificity pocket by forming a protein-ligand-adduct. However, since the S1 pockets of β5c and β5i significantly vary in size (Huber et al., 2012), even slight modifications of the P1 residue promote proteasome specificity.

Further synthetic approaches have centered on more easily synthesizable derivatives of TMC-95A. Replacement of the atropisomeric oxindole-phenyl moiety lead to cyclic peptides composed of a Tyr-Asn-Tyr backbone with an endocyclic biaryl ether (BIA) clamp between the two Tyr P2/P4 side-chains (Kaiser et al., 2004b; Groll et al., 2006b) (Figure 2F). Although the $K_i$-values of the BIA-compounds were shown to be 1000-fold higher compared to TMC-95A, crystallographic data revealed that the natural product's rotationally constrained oxindole-aryl side-chain crosslink is substantial for proper binding into the proteasomal substrate-binding channel.

Other examples of natural peptidic, cyclic CP inhibitors include argyrin A and scytonemide A (Ley et al., 2002; Nickeleit et al., 2008) (Figure 2F). The former exhibits inhibition potencies comparable to bortezomib and was shown to possess anti-tumor activity, however, its mode of action on the CP still has to be elucidated. The cyclic heptapeptide scytonemide A illustrates *in vitro* $IC_{50}$ values in the nanomolar range, but lacks activity in cell-based assays due to its chemical instability (Krunic et al., 2010). To date, there are no CP:argyrin A and CP:scytonemide A crystal structures available that can provide insights into their binding mode.

## Synthetic noncyclic peptides and peptide isosteres without reactive head groups

A second option, besides derivatization of natural products such as TMC-95A, is the *de novo* design of noncyclic peptides and isosteres thereof, which predominantly mimic the binding mode of conventional substrates. In 1998, 5-methoxy-1-indanone-dipeptide benzamides (CVT-659; Figure 2G) were identified as potent, competitive inhibitors of ChTL activity, with $IC_{50}$ values as low as 160 nM (Lum et al., 1998). In the same year, the peptide isostere and HIV protease inhibitor ritonavir was found to selectively inhibit the ChTL activity (André et al., 1998; Schmidtke et al., 1999) (Figure 2G; Table 1). Inspired by the observation of a reversible mode of action, benzylstatine peptides were further investigated with the support of computational modeling studies, ultimately yielding ChTL-specific N- and C-terminally capped dipeptides with $IC_{50}$ values in the nanomolar range (Furet et al., 2004). Recently, capped tripeptides comprising the unnatural amino acid *S*-homo-phenylalanine were presented as a result of a high-throughput screening (HTS) with comparable potency and specificity, including structural evidence from X-ray crystallography (Blackburn et al., 2010). Reiterated optimization of the identified hits resulted in compounds with single-digit nanomolar $IC_{50}$ values (Figure 2G; Table 1). The high affinity is primarily achieved by the neopentyl-Asn P3 residue, which exhibits its proper shape complementary with the S3 specificity pocket, as previously discovered in a study of α-keto-1,3,4-oxadiazoles (Rydzewski et al., 2006). The S4 binding site does not resemble a pocket-like structure and thus cannot be categorized by the general S1–S3 specificity pocket scheme. As a result, a variety of spacious P4 residues can be employed in CP inhibitors, but they hardly contribute to affinity and maintain only unspecific interactions. Nevertheless, evolutionarily optimized natural products such as TMC-95A, epoxomicin, fellutamide B and glidobactin successfully interact with distant CP pockets, employing structures that are certainly not in a medicinal chemists' usual toolbox (Huber and Groll, 2012).

Furthermore, the functional and structural characterization of linear decarboxylated TMC-95A analogues suggested a common principle of peptide ligand binding to proteases (Basse et al., 2007; Groll et al., 2010). As a rule, once the peptide bond is hydrolyzed at a proteolytic center of any kind of protease, product release takes place through repulsion between the nucleophile at the active site and the newly generated carboxyl terminus of

the peptide fragment. TMC-95A and its derivatives lack this repulsive element and therefore might be a promising lead in the development of target-oriented non-covalent protease inhibitors. Thus, optimized decarboxylated peptide fragments can be simply designed to act as subunit-specific CP inhibitors based on the unique cleavage preference of the distinct active sites (Groll et al., 2010). Additionally, most CP:ligand complex structures display a MES molecule in the electron density map derived from the crystallization buffer, which populates the oxyanion hole that is typically occupied by the head groups of covalent inhibitors (Figure 4E). Here, MES stabilizes the linear peptide via Van der Waals interactions and forms a network of hydrogen bonds with the active site Thr1.

Blackburn et al. point out that in contrast to bortezomib, non-covalently acting tripeptides are unable to achieve complete proteasomal inhibition in cancer cells, even at maximum compound concentrations, although the degree of blockage is sufficient to cause antiproliferative effects (Blackburn et al., 2010). Cytotoxicity against healthy cells is therefore unlikely. Interestingly, a correlation of large P1 caps combined with sterically less demanding moieties in P3 was reported regarding selective β5i inhibition. In comparison, β5c-selective peptides bear smaller P1 residues as well as bulkier P3 moieties. This correlation was recently deemed to be in accordance with crystal structure studies of cCP and iCP in complexes with selective inhibitors (Huber et al., 2012).

## Non-peptides targeting previously unobserved binding pockets

The application of biologically active peptides leads to considerable drawbacks, such as chemical and biological instability, poor membrane permeability, rapid plasma clearance and immunogenicity. The overwhelming majority of inhibitors, however, contain peptidic and peptidomimetic structures. Small, non-peptide structures are very desirable, yet few inhibitors feature a completely non-peptidic scaffold.

PI-083, a chloronaphthoquinone that is attached to a pyridinyl benzenesulfonamide (Figure 2I), was discovered by HTS against the CP (Kazi et al., 2009). Molecular modeling studies suggest a non-covalent binding mode, although the authors note that a covalent interaction with Thr1O$^{\gamma}$ cannot be excluded (Lawrence et al., 2010). Subsequent efforts to improve the affinity ($IC_{50}$=1000 nM) by derivatization of the chloronaphthoquinone and sulfonamide moieties were not successful. In a further screening effort, Ge et al. identified hydronaphtoquinones to be novel proteasome inhibitors, which were optimized via extensive SAR-guided development to exhibit $IC_{50}$ values of 150 nM (Ge et al., 2012). Interestingly, a derivative with a three times worse *in vitro* $IC_{50}$ value (440 nM; Figure 2I) was the most active inhibitor for the ChTL activity in intact breast cancer cells, which again demonstrates that results from *in vitro* experiments do not proportionally transfer to effects *in vivo*. Dialysis experiments revealed that the optimized derivative irreversibly inhibits the 20S proteasome, but investigations into the binding mode using computational or crystal structure studies have not been undertaken to date.

Recently, a HTS was performed with a library containing (i) close derivatives of compounds that passed clinical trials and (ii) only non-peptidic structures. As a result, *N*-hydroxyurea-derived compounds were found to be potent, reversible inhibitors of the β5-active site of the CP (Gallastegui et al., 2012) (Figure 2I). Even at 200 μM inhibitor concentration, there was no inhibition of CL and TL active sites observed. X-ray diffraction studies displayed an unexpected novel binding mode, revealing these compounds to be a new class of CP inhibitors and confirming a non-covalent mode of action. While the *N*-hydroxyurea functionality is stabilized by hydrogen bonds to Thr21NH and Thr21O and Gly47O, in analogy to peptide-based inhibitors, the rigid propynylbenzene residue projects towards a hydrophobic S1 subpocket and establishes multiple Van der Waals interactions with it. Furthermore, molecular modeling studies were performed to target an as yet unobserved hydrophobic S3 subpocket formed by amino acids from the adjacent β6 subunit. It was found that this pocket perfectly accommodates an adamantyl moiety, since this residue represents a promising fit with the S3 subpocket. Although the adamantyloxy-equipped inhibitor displayed an $IC_{50}$ value of 780 nM, there is space for additional improvements in the complementary of charged moieties for polar interactions. In the course of hit optimization, small halogenated and extended aliphatic residues at the *meta*-position of the aromatic ring proved to be unfavorable with $IC_{50}$ values in the millimolar range. Removal of the *meta*-substituent results in a complete loss of potency, underlining that the oxygen of the ether group also significantly contributes to stabilization of the ligand (Gallastegui et al., 2012). As expected from the structural results, optimization of the residue at the stereogenic center and enantioselective synthesis further improved the $IC_{50}$ value from 780 nM to 340 nM (HU-10, Figure 2I; Table 1). In contrast, derivatives without the methyl or with ethyl or isopropyl

moieties at the stereocenter displayed a 15-fold decrease in $IC_{50}$, indicating that even small hydrophobic interactions contribute to inhibitor stabilization, although steric clashes with the protein backbone cannot be countervailed. This underlines the urge for precise chemical fine-tuning of non-covalent inhibitors, whereas their covalent counterparts are able to compensate for clashes with protein amino acid side-chains due to strong unspecific binding to the active site nucleophile Thr1.

Interestingly, the *N*-hydroxyurea compounds displayed remarkable rigidity and a tight binding mode, as shown in crystal soaking experiments (Gallastegui et al., 2012). When treated with a racemic mixture, proteasomes in the crystals selected for the *R*-enantiomer. Nevertheless, structural elucidation of the CP with the *S*-conformer revealed that the bound inhibitor structurally superimposes with the 150-fold more potent *R*-enantiomer, except for the methyl group. In view of the non-covalent binding mode, this observation demonstrates that the pharmacophore is bound tightly to the ChTL subunit, though slight changes in the overall structure of the ligand have already resulted in prominent alterations in the $IC_{50}$ values.

Surprisingly, the electron density maps of all CP:*N*-hydroxyurea crystal structures display a MES molecule from the crystallization buffer that occupies the oxyanion hole. This is similar to that observed for the linear decarboxylated TMC-95A derivatives, but in the case of the *N*-hydroxyurea compounds the MES molecule does not show any mutual stabilization. The regularity of the appearance of MES (Figures 3F,4E and 4F) points to the fact that it is a promising fragment that should be further exploited in proteasomal drug development. Due to the plentitude of the covalent and non-covalent binding modes of CP:ligand complex structures, computational modeling approaches might now allow a directed evolutionary approach in the optimization of existing and the design of novel proteasome inhibitors.

## Conclusions

Revisiting the plethora of CP inhibitors, it is obvious that the design of novel compounds from known sets of pharmacophoric elements must be feasible. However, the application of crystallographic information in computational methods remains difficult, as the model of a rigid CP does not reflect structural rearrangements in the proteasomal specificity pockets upon ligand binding. Specificity pockets unexpectedly alter their conformation and even apo- and holo-structures do not serve as a blueprint for the computational prediction of $IC_{50}$ values or binding modes. In addition, the popular assumptions of drug design and methods of modeling/docking studies need to be reiteratively refined so that they resemble the complex chemical processes during peptide degradation (Klebe, 2011). Advances to support *in silico* techniques with solid thermodynamic data from isothermal titration calorimetry remain difficult due to batch size limitations, and methods for the determination of $k_{on}/k_{off}$ rates of ligands are also in dispute.

Dismissal of reactive head groups is a radical but necessary approach for the improvement of the pharmacokinetic and pharmacodynamic profiles of inhibitors. The substantial loss of enthalpic stabilization must then be compensated by exhaustive optimization via non-covalent interactions with the substrate binding channel and structurally constrained molecules that are, nevertheless, difficult to synthesize as demonstrated with synthetic analogues of TMC-95A. The discovery of *N*-hydroxyurea compounds as CP inhibitors with a previously unobserved binding mode proved that opportunities in this field are far from being exhausted. For example, fragment-based drug design approaches have yet to be undertaken as a further source of innovation.

In comparison to other enzymes, the CP is an easy target for initial drug discovery as it has a central role in many metabolic pathways and belongs to the small family of Ntn-hydrolases. Accordingly, CP blockage by irreversible or slowly reversible inhibitors shows immediate responses *in vitro* as well as *in vivo*; nonetheless, persistent shutdown of proteasomal peptide degradation represents serious metabolic interference affecting the viability of both malignant and healthy cells. In contrast, time-limited CP inhibition via non-covalently binding inhibitors is suggested to induce less cytotoxic effects due to a more adequate degree of CP blockage, while still retaining therapeutic effects. To our knowledge, no non-covalent CP inhibitors have been evaluated in clinical phase studies to date, suggesting that promising inhibition profiles *in vitro* could not be transferred to satisfactory effects *in vivo*. The *status quo* reported here therefore demonstrates that in spite of extensive efforts in the field of CP inhibition, there is still room for innovation, for example through fragment-based drug design, to discover new chemical entities. Therefore, academic as well as industrial research faces a formidable, but highly rewarding challenge that will be interesting to follow over the next decade.

Received May 25, 2012; accepted August 12, 2012

## References


Adams, J., Behnke, M., Chen, S., Cruickshank, A.A, Dick, L.R., Grenier, L., Klunder, J.M., Ma, Y.-T., Plamondon, L., and Stein, R.L. (1998). Potent and selective inhibitors of the proteasome: dipeptidyl boronic acids. Bioorg. Med. Chem. Lett. *8*, 333–338.

Adams, J., Palombella, V.J., Sausville, E.A., Johnson, J., Destree, A., Lazarus, D.D., Maas, J., Pien, C.S., Prakash, S., and Elliott, P.J. (1999). Proteasome inhibitors: a novel class of potent and effective antitumor agents proteasome inhibitors. Cancer Res. *59*, 2615–2622.

Albrecht, B.K. and Williams, R.M. (2004). A concise, total synthesis of the TMC-95A/B proteasome inhibitors. PNAS *101*, 11949–11954.

André, P., Groettrup, M., Klenerman, P., de Giuli, R., Booth, B.L., Cerundolo, V., Bonneville, M., Jotereau, F., Zinkernagel, R. M., and Lotteau, V. (1998). An inhibitor of HIV-1 protease modulates proteasome activity, antigen presentation, and T cell responses. PNAS *95*, 13120–13124.

Arastu-Kapur, S., Anderl, J.L., Kraus, M., Parlati, F., Shenk, K.D., Lee, S.J., Muchamuel, T., Bennett, M.K., Driessen, C., Ball, A.J., et al. (2011). Nonproteasomal targets of the proteasome inhibitors bortezomib and carfilzomib: a link to clinical adverse events. Clin. Cancer Res. *17*, 2734–2743.

Asai, A., Hasegawa, A., Ochiai, K., Yamashita, Y., and Mizukami, T. (2000). Belactosin A, a novel antitumor antibiotic acting on cyclin/CDK mediated cell cycle regulation, produced by *Streptomyces* sp. J. Antibiot. (Tokyo). *53*, 81–83.

Asai, A., Tsujita, T., Sharma, S.V., Yamashita, Y., Akinaga, S., Funakoshi, M., Kobayashi, H., and Mizukami, T. (2004). A new structural class of proteasome inhibitors identified by microbial screening using yeast-based assay. Bioche. Pharmacol. *67*, 227–234.

Basler, M., Dajee, M., Moll, C., Groettrup, M., and Kirk, C.J. (2010). Prevention of experimental colitis by a selective inhibitor of the immunoproteasome. J. Immunol. *185*, 634–641.

Basse, N., Piguel, S., Papapostolou, D., Ferrier-Berthelot, A., Richy, N., Pagano, M., Sarthou, P., Sobczak-Thépot, J., Reboud-Ravaux, M., and Vidal, J. (2007). Linear TMC-95-based proteasome inhibitors. J. Med. Chem. *50*, 2842–2850.

Ben-Shem, A., Jenner, L., Yusupova, G., and Yusupov, M. (2010). Crystal structure of the eukaryotic ribosome. Science *330*, 1203–1209.

Berkers, C.R., Verdoes, M., Lichtman, E., Fiebiger, E., Kessler, B.M., Anderson, K.C., Ploegh, H.L., Ovaa, H., and Galardy, P.J. (2005). Activity probe for *in vivo* profiling of the specificity of proteasome inhibitor bortezomib. Nat. Methods *2*, 357–362.

Berthelot, A., Piguel, S., Le Dour, G., and Vidal, J. (2003). Synthesis of macrocyclic peptide analogues of proteasome inhibitor TMC-95A. J. Organic Chem. *68*, 9835–9838.

Bianchi, G., Oliva, L., Cascio, P., Pengo, N., Fontana, F., Cerruti, F., Orsi, A., Pasqualetto, E., Mezghrani, A., Calbi, V., et al. (2009). The proteasome load vs. capacity balance determines apoptotic sensitivity of multiple myeloma cells to proteasome inhibition. Blood *113*, 3040–3049.

Blackburn, C., Gigstad, K.M., Hales, P., Garcia, K., Jones, M., Bruzzese, F.J., Barrett, C., Liu, J.X., Soucy, T.A., Sappal, D.S., et al. (2010). Characterization of a new series of non-covalent proteasome inhibitors with exquisite potency and selectivity for the 20S beta5-subunit. Biochem. J. *430*, 461–476.

Bochtler, M., Ditzel, L., Groll, M., Hartmann, C., and Huber, R. (1999). The proteasome. Ann. Rev. Biophys. Biomol. Struct. *28*, 295–317.

Borissenko, L. and Groll, M. (2007). 20S proteasome and its inhibitors: crystallographic knowledge for drug development. Chem. Rev. *107*, 687–717.

Brannigan, J.A., Dodson, H.J., Moody, P.C.E., Smith, J.L., Tomchick, D.R., and Murzin, A.G. (1995). A protein catalytic framework with an N-terminal nucleophile is capable of self-activation. Nature *378*, 416–419.

Braun, H.A., Umbreen, S., Groll, M., Kuckelkorn, U., Mlynarczuk, I., Wigand, M.E., Drung, I., Kloetzel, P.-M., and Schmidt, B. (2005). Tripeptide mimetics inhibit the 20 S proteasome by covalent bonding to the active threonines. J. Biol. Chem.y *280*, 28394–28401.

Bross, P., Farrell, A., and Pazdur, R. (2003). Velcade(R): U.S. FDA Approval for the treatment of multiple myeloma progressing on prior therapy. Oncologist *8*, 508–513.

Bürgi, H., Dunitz, J., and Shefter, E. (1973). Geometrical reaction coordinates. II. Nucleophilic addition to a carbonyl group. J. Am. Chem. Soc. *587*, 5065–5067.

Cascio, P., Call, M., Petre, B.M., Walz, T., and Goldberg, A.L. (2002). Properties of the hybrid form of the 26S proteasome containing both 19S and PA28 complexes. EMBO J. *21*, 2636–2645.

Chauhan, D., Catley, L., Li, G., Podar, K., Hideshima, T., Velankar, M., Mitsiades, C., Mitsiades, N., Yasui, H., Letai, A., et al. (2005). A novel orally active proteasome inhibitor induces apoptosis in multiple myeloma cells with mechanisms distinct from bortezomib. Cancer Cell *8*, 407–419.

Chauhan, D., Singh, A.V., Aujay, M., Kirk, C.J., Bandi, M., Ciccarelli, B., Raje, N., Richardson, P., and Anderson, K. C. (2010). A novel orally active proteasome inhibitor ONX 0912 triggers *in vitro* and *in vivo* cytotoxicity in multiple myeloma. Blood *116*, 4906–4915.

Chauhan, D., Tian, Z., Zhou, B., Kuhn, D., Orlowski, R., Raje, N., Richardson, P., and Anderson, K.C. (2011). In vitro and *in vivo* selective antitumor activity of a novel orally bioavailable proteasome inhibitor MLN9708 against multiple myeloma cells. Clin. Caner Res. *17*, 5311–5321.

Craiu, A., Gaczynska, M., Akopian, T., Gramm, C.F., Fenteany, G., Goldberg, A.L., and Rock, K.L. (1997). Lactacystin and clasto-lactacystin β-lactone modify multiple proteasome β-subunits and inhibit intracellular protein degradation and major histocompatibility complex class I antigen presentation. J. Biol. Chem. *272*, 13437–13445.

Demo, S.D., Kirk, C.J., Aujay, M.A., Buchholz, T.J., Dajee, M., Ho, M.N., Jiang, J., Laidig, G.J., Lewis, E.R., Parlati, F., et al. (2007). Antitumor activity of PR-171, a novel irreversible inhibitor of the proteasome. Cancer Res. *67*, 6383–6391.

Dick, L.R., Cruikshank, A.A., Destree, A.T., Grenier, L., McCormack, T.A., Melandri, F.D., Nunes, S.L., Palombella, V.J., Parent, L.A., Plamondon, L., et al. (1997). Mechanistic studies on the inactivation of the proteasome by lactacystin in cultured cells. J. Biol. Chem. *272*, 182–188.

Dorsey, B.D., Iqbal, M., Chatterjee, S., Menta, E., Bernardini, R., Bernareggi, A., Cassarà, P.G., D'Arasmo, G., Ferretti, E., De Munari, S., et al. (2008). Discovery of a potent, selective, and orally active proteasome inhibitor for the treatment of cancer. J. Med. Chem. *51*, 1068–1072.

Driscoll, J., Brown, M., and Finley, D. (1993). MHC-linked LMP gene products specifically alter peptidase activities of the proteasome. Nature *365*, 262–264.

Feling, R.H., Buchanan, G.O., Mincer, T.J., Kauffman, C.A., Jensen, P.R., and Fenical, W. (2003). Salinosporamide A: a highly cytotoxic proteasome inhibitor from a novel microbial source, a marine bacterium of the new genus *Salinospora*. Angew. Chem. Int. Ed. Engl. *42*, 355–357.

Fenteany, G., Standaert, R.F., Lane, W.S., Choi, S., Corey, E.J., and Schreiber, S.L. (1995). Inhibition of proteasome activities and subunit-specific amino-terminal threonine modification by lactacystin. Science *268*, 726–731.

Figueiredo-Pereira, M.E., Berg, K.A., and Wilk, S. (1994). A new inhibitor of the chymotrypsin-like activity of the multicatalytic proteinase complex (20S proteasome) induces accumulation of ubiquitin-protein conjugates in a neuronal cell. J. Neurochem. *63*, 1578–1581.

Franke, N.E., Niewerth, D., Assaraf, Y.G., van Meerloo, J., Vojtekova, K., van Zantwijk, C.H., Zweegman, S., Chan, E.T., Kirk, C.J., Geerke, D.P., et al. (2012). Impaired bortezomib binding to mutant β5 subunit of the proteasome is the underlying basis for bortezomib resistance in leukemia cells. Leukemia *26*, 757–768.

Furet, P., Imbach, P., Noorani, M., Koeppler, J., Laumen, K., Lang, M., Guagnano, V., Fuerst, P., Roesel, J., Zimmermann, J., et al. (2004). Entry into a new class of potent proteasome inhibitors having high antiproliferative activity by structure-based design. J. Med. Chem. *47*, 4810–4813.

Gallastegui, N. and Groll, M. (2010). The 26S proteasome: assembly and function of a destructive machine. Trends Biochem. Sci. *35*, 634–642.

Gallastegui, N., Beck, P., Arciniega, M., Huber, R., Hillebrand, S., and Groll, M. (2012). Hydroxyureas as noncovalent proteasome inhibitors. Angew. Chem. Int. Ed. Engl. *51*, 247–249.

Ge, Y., Kazi, A., Marsilio, F., Luo, Y., Jain, S., Brooks, W., Daniel, K.G., Guida, W.C., Sebti, S.M., and Lawrence, H.R. (2012). Discovery and synthesis of hydronaphthoquinones as novel proteasome inhibitors. J. Med. Chem. *55*, 1978–1998.

Groettrup, M., Kraft, R., Kostka, S., Standera, S., Stohwasser, R., and Kloetzel, P.-M. (1996). A third interferon-γ-induced subunit exchange in the 20S proteasome. Eur. J. Immunol. *26*, 863–869.

Groll, M. and Huber, R. (2003). Substrate access and processing by the 20S proteasome core particle. Int. J. Biochem. Cell Biol. *35*, 606–616.

Groll, M. and Potts, B.C. (2011). Proteasome structure, function, and lessons learned from β-lactone inhibitors. Curr. Top. Med. Chem. *11*, 2850–2878.

Groll, M., Ditzel, L., Lowe, J., Stock, D., Bochtler, M., Bartunik, H.D., and Huber, R. (1997). Structure of 20S proteasome from yeast at 2.4 resolution. Nature *386*, 463–471.

Groll, M., Kim, K.B., Kairies, N., Huber, R., and Crews, C. M. (2000). Crystal structure of epoxomicin:20S proteasome reveals a molecular basis for selectivity of α′,β′-epoxyketone proteasome inhibitors. J. Am. Chem. Soc. *122*, 1237–1238.

Groll, M., Koguchi, Y., Huber, R., and Kohno, J. (2001). Crystal structure of the 20 S proteasome:TMC-95A complex: a non-covalent proteasome inhibitor. J. Mol. Biol. *311*, 543–548.

Groll, M., Nazif, T., Huber, R., and Bogyo, M. (2002). Probing structural determinants distal to the site of hydrolysis that control substrate specificity of the 20S proteasome. Chem. Biol. *9*, 655–662.

Groll, M., Berkers, C.R., Ploegh, H.L., and Ovaa, H. (2006a). Crystal structure of the boronic acid-based proteasome inhibitor bortezomib in complex with the yeast 20S proteasome. Structure *14*, 451–456.

Groll, M., Götz, M., Kaiser, M., Weyher, R., and Moroder, L. (2006b). TMC-95-based inhibitor design provides evidence for the catalytic versatility of the proteasome. Chem. Biol. *13*, 607–614.

Groll, M., Huber, R., and Potts, B.C.M. (2006c). Crystal structures of Salinosporamide A (NPI-0052) and B (NPI-0047) in complex with the 20S proteasome reveal important consequences of β-lactone ring opening and a mechanism for irreversible binding. J. Am. Chem. Soc. *128*, 5136–5141.

Groll, M., Larionov, O. V., Huber, R., and de Meijere, A. (2006d). Inhibitor-binding mode of homobelactosin C to proteasomes: new insights into class I MHC ligand generation. PNAS *103*, 4576–4579.

Groll, M., Schellenberg, B., Bachmann, A.S., Archer, C.R., Huber, R., Powell, T.K., Lindow, S., Kaiser, M., and Dudler, R. (2008). A plant pathogen virulence factor inhibits the eukaryotic proteasome by a novel mechanism. Nature *452*, 755–758.

Groll, M., Huber, R., and Moroder, L. (2009). The persisting challenge of selective and specific proteasome inhibition. J. Peptide Sci. *15*, 58–66.

Groll, M., Gallastegui, N., Maréchal, X., Le Ravalec, V., Basse, N., Richy, N., Genin, E., Huber, R., Moroder, L., Vidal, J., et al. (2010). 20S proteasome inhibition: designing noncovalent linear peptide mimics of the natural product TMC-95A. Chem. Med. Chem. *5*, 1701–1705.

Gräwert, M.A., Gallastegui, N., Stein, M., Schmidt, B., Kloetzel, P.-M., Huber, R., and Groll, M. (2011). Elucidation of the α-keto-aldehyde binding mechanism: a lead structure motif for proteasome inhibition. Angew. Chem. Int. Ed. Engl. *50*, 542–544.

Hanada, M., Sugawara, K., Kaneta, K., Toda, S., Nishiyama, Y., Tomita, K., Yamamoto, H., Konishi, M., and Oki, T. (1992). Epoxomicin, a new antitumor agent of microbial origin. J. Antibiot. (Tokyo). *45*, 1746–1752.

Harding, C.V., France, J., Song, R., Farah, J.M., Chatterjee, S., and Chester, W. (1995). Novel dipeptide aldehydes are proteasome inhibitors and block the MHC-I antigen-processing pathway. J. immunol. *155*, 1767–1775.

Hershko, A. and Ciechanover, A. (1998). The ubiquitin system. Ann. Rev. Biochem. *67*, 425–479.

Hines, J., Groll, M., Fahnestock, M., and Crews, C. M. (2008). Proteasome inhibition by fellutamide B induces nerve growth factor synthesis. Chem. Biol. *15*, 501–512.

Huber, E.M. and Groll, M. (2012). Inhibitors for the immuno- and constitutive proteasome: current and future trends in drug development. Angew. Chem. Int. Ed. Engl. *51*, 8708–8720,

Huber, E.M., Basler, M., Schwab, R., Heinemeyer, W., Kirk, C.J., Groettrup, M., and Groll, M. (2012). Immuno- and constitutive

proteasome crystal structures reveal differences in substrate and inhibitor specificity. Cell *148*, 727–738.

Ichikawa, H.T., Conley, T., Muchamuel, T., Jiang, J., Lee, S., Owen, T., Barnard, J., Nevarez, S., Goldman, B.I., Kirk, C.J., et al. (2011). Novel proteasome inhibitors have a beneficial effect in murine lupus via the dual inhibition of type i interferon and autoantibody secreting cells. Arthritis Rheum. *64*, 493–503.

Kaiser, M., Groll, M., Renner, C., Huber, R., and Moroder, L. (2002). The core structure of TMC-95A is a promising lead for reversible proteasome inhibition. Angew. Chem. Int. Ed. Engl. *41*, 780–783.

Kaiser, M., Siciliano, C., Assfalg-Machleidt, I., Groll, M., Milbradt, A.G., and Moroder, L. (2003). Synthesis of a TMC-95A ketomethylene analogue by cyclization via intramolecular Suzuki coupling. Org. Lett. *5*, 3435–3437.

Kaiser, M., Groll, M., Siciliano, C., Assfalg-Machleidt, I., Weyher, E., Kohno, J., Milbradt, A.G., Renner, C., Huber, R., and Moroder, L. (2004a). Binding mode of TMC-95A analogues to eukaryotic 20S proteasome. Chem. Bio. Chem. *5*, 1256–1266.

Kaiser, M., Milbradt, A., Siciliano, C., Assfalg-Machleidt, I., Machleidt, W., Groll, M., Renner, C., and Moroder, L. (2004b). TMC-95A analogues with endocyclic biphenyl ether group as proteasome inhibitors. Chem. Biodivers. *1*, 161–173.

Kane, R.C., Dagher, R., Farrell, A., Ko, C.-W., Sridhara, R., Justice, R., and Pazdur, R. (2007). Bortezomib for the treatment of mantle cell lymphoma. Clin. Cancer Res. *13*, 5291–5294.

Kazi, A., Lawrence, H., Guida, W.C., McLaughlin, M.L., Springett, G.M., Berndt, N., Yip, R.M.L., and Sebti, S.M. (2009). Discovery of a novel proteasome inhibitor selective for cancer cells over non-transformed cells. Cell Cycle *8*, 1940–1951.

Kisselev, A.F. and Goldberg, A.L. (2001). Proteasome inhibitors: from research tools to drug candidates. Chem. Biol. *8*, 739–758.

Klebe, G. (2011). On the validity of popular assumptions in computational drug design. J. Cheminform. *3*, O18.

Koguchi, Y., Kohno, J., Nishio, M., Takagashi, K., Okuda, T., Ohnuki, T., and Komatsubara, S. (2000). TMC-95A, B, C, and D, novel proteasome inhibitors produced by Apiospora montagnei Sacc. TC 1093. Taxonomy, production, isolation, and biological activities. J. Antibiot. (Tokyo). *53*, 105–109.

Korotkov, V.S., Ludwig, A., Larionov, O.V., Lygin, A.V., Groll, M., and de Meijere, A. (2011). Synthesis and biological activity of optimized belactosin C congeners. Org. Biomol. Chem. *9*, 7791–7798.

Krunic, A., Vallat, A., Mo, S., Lantvit, D.D., Swanson, S.M., and Orjala, J. (2010). Scytonemides A and B, cyclic peptides with 20S proteasome inhibitory activity from the cultured cyanobacterium *Scytonema hofmanii*. J. Nat. Prod. *73*, 1927–1932.

Kuhn, D., Orlowski, R., and Bjorklund, C. (2011). Second generation proteasome inhibitors: Carfilzomib and immunoproteasome-specific inhibitors (IPSIs). Curr. Cancer Drug Targets *11*, 285–295.

Kumar, S.K., Lee, J.H., Lahuerta, J.J., Morgan, G., Richardson, P.G., Crowley, J., Haessler, J., Feather, J., Hoering, A., Moreau, P., et al. (2012). Risk of progression and survival in multiple myeloma relapsing after therapy with IMiDs and bortezomib: a multicenter international myeloma working group study. Leukemia *26*, 149–157.

Kupperman, E., Lee, E.C., Cao, Y., Bannerman, B., Fitzgerald, M., Berger, A., Yu, J., Yang, Y., Hales, P., Bruzzese, F., et al. (2010). Evaluation of the proteasome inhibitor MLN9708 in preclinical models of human cancer. Cancer Res. *70*, 1970–1980.

Lawrence, H.R., Kazi, A., Luo, Y., Kendig, R., Ge, Y., Jain, S., Daniel, K., Santiago, D., Guida, W.C., and Sebti, S.M. (2010). Synthesis and biological evaluation of naphthoquinone analogs as a novel class of proteasome inhibitors. Bioorg. Med. Chem. *18*, 5576–5592.

Ley, S.V., Priour, A., and Heusser, C. (2002). Total synthesis of the cyclic heptapeptide Argyrin B: a new potent inhibitor of T-cell independent antibody formation. Org. Lett. *4*, 711–714.

Lin, S. and Danishefsky, S.J. (2002). The total synthesis of proteasome inhibitors TMC-95A and TMC-95B: discovery of a new method to generate cis-propenyl amides. Angew. Chem. Int. Ed. Engl. *41*, 512–515.

Lin, S., Yang, Z.-Q., Kwok, B.H.B., Koldobskiy, M., Crews, C.M., and Danishefsky, S.J. (2004). Total synthesis of TMC-95A and -B via a new reaction leading to Z-enamides. Some preliminary findings as to SAR. J. Am. Chem. Soc. *126*, 6347–6355.

Lin, G., Li, D., de Carvalho, L.P.S., Deng, H., Tao, H., Vogt, G., Wu, K., Schneider, J., Chidawanyika, T., Warren, J.D., et al. (2009). Inhibitors selective for mycobacterial versus. human proteasomes. Nature *461*, 621–626.

Loidl, G., Groll, M., Musiol, H.J., Ditzel, L., Huber, R., and Moroder, L. (1999a). Bifunctional inhibitors of the trypsin-like activity of eukaryotic proteasomes. Chem. Biol. *6*, 197–204.

Loidl, G., Groll, M., Musiol, H.J., Huber, R., and Moroder, L. (1999b). Bivalency as a principle for proteasome inhibition. PNAS *96*, 5418–5422.

Löwe, J., Stock, D., Jap, B., Zwickl, P., Baumeister, W., and Huber, R. (1995). Crystal structure of the 20S proteasome from the archaeon T. acidophilum at 3.4 Å resolution. Science *268*, 533–539.

Lum, R.T., Nelson, M.G., Joly, A., Horsma, A.G., Lee, G., Meyer, S.M., Wick, M.M., and Schow, S.R. (1998). Selective inhibition of the chymotrypsin-like activity of the 20S proteasome by 5-methoxy-1-indanone dipeptide benzamides. Bioorg. Med. Chem. Lett. *8*, 209–214.

Lynas, J.F., Harriott, P., Healy, A., McKervey, M.A., and Walker, B. (1998). Inhibitors of the chymotrypsin-like activity of proteasome based on di- and tri-peptidyl α-keto aldehydes (glyoxals). Bioorg. Med. Chem. Lett. *8*, 373–378.

Macherla, V.R., Mitchell, S.S., Manam, R.R., Reed, K.A., Chao, T.H., Nicholson, B., Deyanat-Yazdi, G., Mai, B., Jensen, P.R., Fenical, W.F., et al. (2005). Structure-activity relationship studies of salinosporamide A (NPI-0052), a novel marine derived proteasome inhibitor. J. Med. Chem. *48*, 3684–3687.

Maldonado, L.A., Fenical, W., Jensen, P.R., Kauffman, C.A., Mincer, T.J., Ward, A.C., Bull, A.T., and Goodfellow, M. (2005). *Salinispora arenicola* gen. nov., sp. nov. and *Salinispora tropica* sp. nov., obligate marine actinomycetes belonging to the family Micromonosporaceae. Int. J. System. Evol. Microbiol. *55*, 1759–1766.

Manam, R.R., McArthur, K.A., Chao, T.-H., Weiss, J., Ali, J.A., Palombella, V.J., Groll, M., Lloyd, G.K., Palladino, M.A., Neuteboom, S.T.C., et al. (2008). Leaving groups prolong the duration of 20S proteasome inhibition and enhance the potency of salinosporamides. J. Med. Chem. *51*, 6711–6724.

Meng, L., Mohan, R., Kwok, B.H.B., Elofsson, M., Sin, N., and Crews, C.M. (1999). Epoxomicin, a potent and selective proteasome inhibitor, exhibits *in vivo* antiinflammatory activity. PNAS *96*, 10403–10408.

Momose, I., Sekizawa, R., Hirosawa, S., Ikeda, D., Naganawa, H., Iinuma, H., and Takeuchi, T. (2001). Tyropeptins A and B, new proteasome inhibitors produced by *Kitasatospora* sp. MK993-dF2. II. Structure determination and synthesis. J. Antibiot. (Tokyo). *54*, 1004–1012.

Momose, I., Umezawa, Y., Hirosawa, S., Iijima, M., Iinuma, H., and Ikeda, D. (2005). Synthesis and activity of tyropeptin A derivatives as potent and selective inhibitors of mammalian 20S proteasome. Biosci. Biotech. Biochem. *69*, 1733–1742.

Muchamuel, T., Basler, M., Aujay, M.A., Suzuki, E., Kalim, K.W., Lauer, C., Sylvain, C., Ring, E.R., Shields, J., Jiang, J., et al. (2009). A selective inhibitor of the immunoproteasome subunit LMP7 blocks cytokine production and attenuates progression of experimental arthritis. Nat. Med. *15*, 781–787.

Murata, S., Sasaki, K., Kishimoto, T., Niwa, S.-I., Hayashi, H., Takahama, Y., and Tanaka, K. (2007). Regulation of $CD8^+$ T cell development by thymus-specific proteasomes. Science *316*, 1349–1353.

Nawrocki, S.T., Carew, J.S., Dunner, K., Boise, L.H., Chiao, P.J., Huang, P., Abbruzzese, J.L., and McConkey, D.J. (2005). Bortezomib inhibits PKR-like endoplasmic reticulum (ER) kinase and induces apoptosis via ER stress in human pancreatic cancer cells. Cancer Res. *65*, 11510–11519.

Nazif, T. and Bogyo, M. (2001). Global analysis of proteasomal substrate specificity using positional-scanning libraries of covalent inhibitors. PNAS *98*, 2967–2972.

Nickeleit, I., Zender, S., Sasse, F., Geffers, R., Brandes, G., Sörensen, I., Steinmetz, H., Kubicka, S., Carlomagno, T., Menche, D., et al. (2008). Argyrin A reveals a critical role for the tumor suppressor protein p27(kip1) in mediating antitumor activities in response to proteasome inhibition. Cancer Cell *14*, 23–35.

Nussbaum, A.K., Dick, T.P., Keilholz, W., Schirle, M., Stevanović, S., Dietz, K., Heinemeyer, W., Groll, M., Wolf, D.H., Huber, R., et al. (1998). Cleavage motifs of the yeast 20S proteasome β subunits deduced from digests of enolase 1. PNAS *95*, 12504–12509.

Orlowski, M., Cardozo, C., and Michaud, C. (1993). Evidence for the presence of five distinct proteolytic components in the pituitary multicatalytic proteinase complex. Properties of two components cleaving bonds on the carboxyl side of branched chain and small neutral amino acids. Biochemistry *32*, 1563–1572.

Palombella, V.J., Rando, O.J., Goldberg, A.L., and Maniatis, T. (1994). The ubiquitin-proteasome pathway is required for processing the NF-κB1 precursor protein and the activation of NF-κB. Cell *78*, 773–785.

Piva, R., Ruggeri, B., Williams, M., Costa, G., Tamagno, I., Ferrero, D., Giai, V., Coscia, M., Peola, S., Massaia, M., et al. (2008). CEP-18770: a novel, orally active proteasome inhibitor with a tumor-selective pharmacologic profile competitive with bortezomib. Blood *111*, 2765–2775.

Prudhomme, J., McDaniel, E., Ponts, N., Bertani, S., Fenical, W., Jensen, P., and Le Roch, K. (2008). Marine actinomycetes: a new source of compounds against the human malaria parasite. PloS ONE *3*, e2335.

Rammensee, H.-G., Friede, T., and Stevanovic, S. (1995). MHC ligands and peptide motifs: first listing. Immunogenetics *41*, 178–228.

Rock, K.L. and Goldberg, A.L. (1999). Degradation of cell proteins and the generation of MHC class I-presented peptides. Ann. Rev. Immunol. *17*, 739–779.

Rydzewski, R.M., Burrill, L., Mendonca, R., Palmer, J.T., Rice, M., Tahilramani, R., Bass, K.E., Leung, L., Gjerstad, E., Janc, J.W., et al. (2006). Optimization of subsite binding to the beta5 subunit of the human 20S proteasome using vinyl sulfones and 2-keto-1,3,4-oxadiazoles: syntheses and cellular properties of potent, selective proteasome inhibitors. J. Med. Chem. *49*, 2953–2968.

Schmidtke, G., Kraft, R., Kostka, S., Henklein, P., Frömmel, C., Löwe, J., Huber, R., Kloetzel, P.M., and Schmidt, M. (1996). Analysis of mammalian 20S proteasome biogenesis: the maturation of β-subunits is an ordered two-step mechanism involving autocatalysis. EMBO J. *15*, 6887–6898.

Schmidtke, G., Holzhu, H.-G., Bogyo, M., Kairies, N., Groll, M., Giuli, R. D., Emch, S., and Groettrup, M. (1999). How an inhibitor of the HIV-I protease modulates proteasome activity. Biochemistry *274*, 35734–35740.

Seemüller, E., Lupas, A., Stock, D., Löwe, J., Huber, R., and Baumeister, W. (1995). Proteasome from *Thermoplasma acidophilum:* a threonine protease. Science *268*, 579–582.

Sun, J., Nam, S., Lee, C.-S., and Sebti, S.M. (2001). CEP1612, a dipeptidyl proteasome inhibitor, induces p21 WAF1 and p27 KIP1 expression and apoptosis and inhibits the growth of the human lung adenocarcinoma A-549 in nude mice. Cancer Res. *15,* 1280–1284.

Vinitsky, A., Michaud, C., Powers, J.C., and Orlowski, M. (1992). Inhibition of the chymotrypsin-like activity of the pituitary multicatalytic proteinase complex. Biochemistry *31*, 9421–9428.

Voorhees, P.M., Dees, E.C., Neil, B.O., and Orlowski, R.Z. (2003). The proteasome as a target for cancer therapy. Clin. Cancer Res. *9*, 6316–6325.

Wilk, S. and Orlowski, M. (1983). Evidence that pituitary cation-sensitive neutral endopeptidase is a multicatalytic protease complex. J. Neurochem. *40*, 842–849.

Yang, Z.-Q., Kwok, B.H.B., Lin, S., Koldobskiy, M.A., Crews, C.M., and Danishefsky, S.J. (2003). Simplified synthetic TMC-95A/B analogues retain the potency of proteasome inhibitory activity. Chem. Bio. Chem. *4*, 508–513.

Zhou, H.-J., Aujay, M.A., Bennett, M.K., Dajee, M., Demo, S.D., Fang, Y., Ho, M.N., Jiang, J., Kirk, C.J., Laidig, G.J., et al. (2009). Design and synthesis of an orally bioavailable and selective peptide epoxyketone proteasome inhibitor (PR-047). J. Med. Chem. *52*, 3028–3038.

Philipp Beck studied Molecular Life Sciences at the Friedrich-Alexander-University of Erlangen-Nuremberg. He received his Master of Science degree in 2010 for studies towards the design and synthesis of chiral ligands for metal-catalyzed reactions under the supervision of Profs. Paul Keller and Tim Clark, funded by the Deutscher Akademischer Austauschdienst. For his postgraduate studies he joined the lab of Prof. Groll at the Technische Universität München, where he is currently working on the design and characterization of reversible proteasome inhibitors.

Christian Dubiella, born 1984 in Böblingen (Germany), studied chemistry at the Technische Universität München and received his Master of Science degree in 2011 for crystallographic and biochemical studies on reversible proteasome inhibition under the supervision of Prof. Groll. Currently, he is continuing his research as a PhD student in the group of Prof. Groll focusing on the design and characterization of proteasome inhibitors.

Michael Groll studied chemistry and received his PhD for crystallographic and biochemical studies on the yeast 20S proteasome. After postdoctoral studies in the groups of Prof. Huber (Munich), Prof. Finley (Boston), Prof. Neupert (Munich), and Prof. Kloetzel (Berlin) he became assistant professor at the Charité (Berlin) in 2006. Since 2007, he has been a full professor of biochemistry at the Technische Universität München. His major research interest focuses on the structural and functional characterization of multiprotein complexes.